JACS
JOURNAL OF THE AMERICAN CHEMICAL SOCIETY
Cite This: J. Am. Chem. Soc. 2018, 140, 9001−9019
Perspective
pubs.acs.org/JACS

Semiconductor Nanomembrane Materials for High-Performance Soft Electronic Devices

Mikayla A. Yoder,[†,‡] Zheng Yan,[§] Mengdi Han,[∥] John A. Rogers,[*,‡,∥] and Ralph G. Nuzzo[*,†,‡,⊥]

[†]School of Chemical Sciences, University of Illinois at Urbana−Champaign, Urbana, Illinois 61801, United States

[‡]Frederick Seitz Materials Research Laboratory and Department of Materials Science and Engineering, University of Illinois at Urbana−Champaign, Urbana, Illinois 61801, United States

[§]Department of Chemical Engineering and Department of Mechanical & Aerospace Engineering, University of Missouri, Columbia, Missouri 65211, United States

[∥]Center for Bio-Integrated Electronics, Northwestern University, Evanston, Illinois 60208, United States

[⊥]Surface and Corrosion Science, School of Engineering Sciences in Chemistry, Biotechnology and Health, KTH Royal Institute of Technology, Drottning Kristinas väg 51, SE-100 44 Stockholm, Sweden

ABSTRACT: The development of methods to synthesize and physically manipulate extremely thin, single-crystalline inorganic semiconductor materials, so-called nanomembranes, has led to an almost explosive growth of research worldwide into uniquely enabled opportunities for their use in new "soft" and other unconventional form factors for high-performance electronics. The unique properties that nanomembranes afford, such as their flexibility and lightweight characteristics, allow them to be integrated into electronic and optoelectronic devices that, in turn, adopt these unique attributes. For example, nanomembrane devices are able to make conformal contact to curvilinear surfaces and manipulate strain to induce the self-assembly of various 3D nano/micro device architectures. Further, thin semiconductor materials (e.g., Si-nanomembranes, transition metal dichalcogenides, and phosphorene) are subject to the impacts of quantum and other size-dependent effects that in turn enable the manipulation of their bandgaps and the properties of electronic and optoelectronic devices fabricated from them. In this Perspective, nanomembrane synthesis techniques and exemplary applications of their use are examined. We specifically describe nanomembrane chemistry exploiting high-performance materials, along with precise/high-throughput techniques for their manipulation that exemplify their growing capacities to shape outcomes in technology. Prominent challenges in the chemistry of these materials are presented along with future directions that might guide the development of next generation nanomembrane-based devices.

1. INTRODUCTION

Advances in electronics technology traditionally focus on the miniaturization of circuitry to afford faster, more efficient devices. These advances increasingly exploit active materials in complex thin-film forms while relying on larger device-level structural components to both support and integrate them.[1−4] By reducing not only the lateral dimensions but also thicknesses of full devices, new forms of function can be realized that would otherwise not be possible with bulk materials. Semiconductor nanomembranes (NMs) embody a class of materials that enable such new forms of functionality including capacities for flexure,[1,5] transient construction with tunable paths of degradation,[6,7] transparency,[8−11] strain-engineering from lattice mismatch,[12−16] and tunable bandgaps via quantum confinement effects.[17−19] The term NM encompasses here not only a class of materials rigorously defined by nanoscale thickness but also ranges from atomically thin films to continuous, self-supporting films that have properties independent of their supporting substrates. These functionalities can be exploited to fabricate unique electronic and optoelectronic devices that provide pathways into next-generation electronics.

One important aspect of semiconductor NMs is that they make it possible to use single-crystalline inorganic materials as are generally necessary for high-performance electrical properties while affording unique attributes, such as that of flexure.[1,2,5] Alternative materials as might be used for flexible electronics (e.g., molecular and polymeric organic semiconductors) are generally characterized by carrier mobilities that greatly limit device-level performance characteristics.[5,20] In this Perspective, we highlight progress being made in the chemistry of inorganic NM materials as a distinct class of unconventional solid thin films that harbor a potential for applications within high-performance devices. NMs fabricated using wafer-sourced electronic grade semiconductors, silicon (Si) and III-V compound semiconductors such as GaAs as exemplars, are discussed and compared with more recently emerging 2D NM materials (i.e., atomic thicknesses) as exemplified by the transition metal dichalcogenides (TMDs),[11,17,21] black phosphorus (BP),[19,22] and silicene.[23,24] The former comprises materials that are used in thin film forms that are thicker than a 2D homologue. They exemplify functional materials that have been well-studied and for which established processing techniques can be utilized to both fabricate and integrate them within devices, with understood pathways for optimization and potential for large scale manufacturing. In comparison, 2D NMs are a relatively new class of atomically thin, layered material that have attracted

Received: April 20, 2018
Published: June 27, 2018

DOI: 10.1021/jacs.8b04225
J. Am. Chem. Soc. 2018, 140, 9001−9019

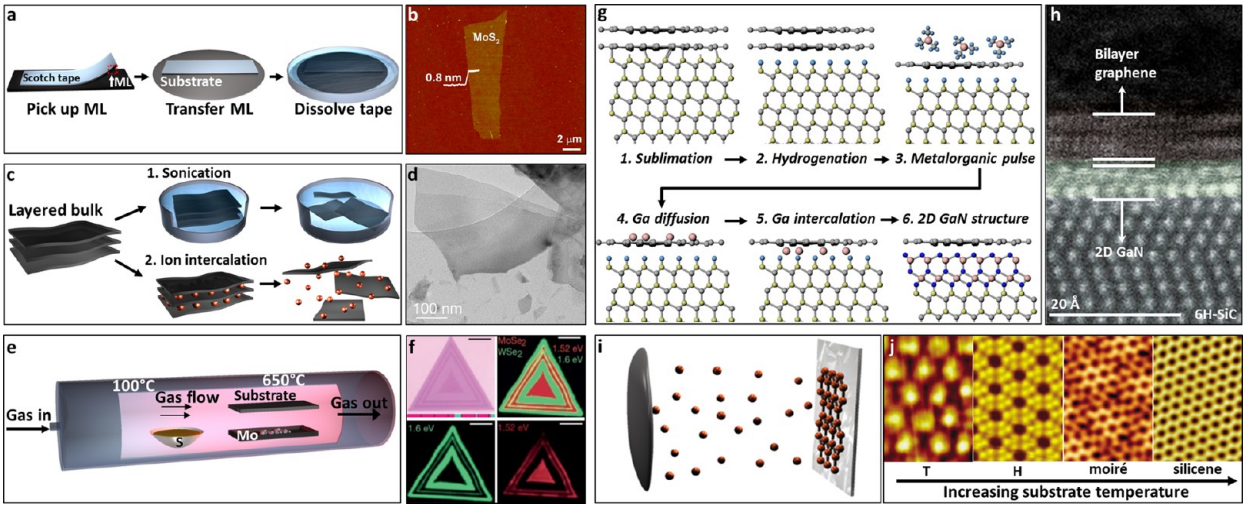

Figure 1. Methods of fabrication for 2D materials. (a) ME schematic of a ML of material and (b) corresponding AFM image of an exfoliated MoS_2 ML.[70] (c) LPE schematic via sonication (top) and Li^+ ion intercalation (bottom) and (d) corresponding TEM image of a MoS_2 flake exfoliated via sonication.[101] (e) Schematic of a CVD process to prepare MoS_2 sheets. (f) Optical image of $MoSe_2/WSe_2$ heterostructure (top left) and photoluminescence maps of $MoSe_2$ (red, bottom right), WSe_2 (green, bottom left), and the $MoSe_2/WSe_2$ heterostructure (top right). Scale bars, 10 μm.[147] (g) GaN synthesis schematic (left) and HAADF-STEM cross-section of 2D GaN (right).[157] (h) Schematic of thermal evaporation of silicene (left) and evolving structures (right).[162] Reproduced from ref 70, 162 with permission from ACS, ref 101 from AAAS, ref 147, 157 from Springer Nature.

considerable attention in consequence of the new possibilities for functional properties they engender, albeit with major requirements remaining for improved methods for their use within devices. It is now well appreciated that NM materials enable new figures of merit for functional performance that are of interest for wearable electronics,[25−27] flexible displays,[28,29] low-cost high-mobility transistors,[30,31] nanoelectronics,[8,32−39] and 3D scaffolds for integration of cellular tissues.[40−43] Of most note is that, with suitable methods of synthesis and processing, such functionalities can be developed in ultrathin materials while retaining the superior qualities associated with electronic and optoelectronic grade source materials.

The following sections highlight recent progress made in the fabrication/synthesis, chemical modification, and application of emerging classes of NM materials in advanced devices: a discussion highlighting the unique attributes of structure and function that their properties facilitate. We first describe the synthesis of 2D NMs, and follow with an overview of methods used for more extended thin film forms, as exemplified by those composed by Si and epitaxial/compound NMs. We follow this with an overview of the construction of devices embracing both 2D and 3D design rules. We conclude with thoughts regarding the current development of the field and suggest important challenges and opportunities for progress that remain to be addressed in research.

2. FABRICATION STRATEGIES FOR SEMICONDUCTOR NANOMEMBRANES

There has been significant attention given to the chemistry of ultrathin and 2D nanomaterials (examples of which are shown in Figures 1 and 2) and procedures for their fabrication and characterization have been extensively reviewed.[1−3,5,11,15,17,19,21,23,24,44−50] In general terms, three distinct, yet variously interrelated, approaches exist for the preparation of NM materials. The most frequently exploited of these methods for 2D NMs follows inspirations afforded by graphene, where an intrinsically layered bulk material (graphite in the case of graphene) is subjected to physical/chemical processing steps to separate discrete NM thin films. Mechanical and chemical exfoliation are the most common methods exploited to do so.[11,17,19,51,52] The second conceptual approach is based on direct chemical growth of the NM material using a supporting substrate from which it can be subsequently separated. This latter approach has been perfected and scaled in industrially relevant processes to produce rolls of graphene on the meter scale. The most advanced method uses Cu foil substrates, providing a fully scalable source for high-quality graphene films reaching to hundreds of meters in length.[53−59] Direct growth of other 2D NMs, however, remains less well developed and restricted to the use of rigid/expensive substrates. In a third conceptual approach, physicochemical processing steps are used to reduce the thicknesses of/or section single-crystalline materials down to very low limiting values: etching, polishing, and selective cutting comprise relevant processing methods used to this end.[8,60−62]

The synthetic method of choice for use in a specific application depends in large measure on the requirements for performance. The use of extractive processing is particularly beneficial for high-performance electronics when single-crystalline wafer sources are readily available along with processing methods for their conversion to NM forms that allow new functionalities, such as extreme mechanical flexibility, and useful approaches to heterogeneous integration.[5,31,48,63−65]

Layered Materials as Precursors for 2D NMs. Crystalline compounds composed of inherently layered structures are nearly ideal source materials for 2D NMs. These materials consist of strong in-plane covalent bonds, with adjacent layers held together by weaker van der Waals (VDW) forces. Many of these so-called graphene-like materials (GLMs) can be exfoliated while maintaining their in-plane crystalline structures. Electrons are generally confined within the 2D atomic planes of these materials and for this reason afford interesting alternatives to single-crystalline materials

DOI: 10.1021/jacs.8b04225
J. Am. Chem. Soc. 2018, 140, 9001−9019

whose ultrathin structures would otherwise be terminated by dangling bonds.[45] Here, much attention has been given to TMDs with compositions in the form of MX_2 (where M is a transition metal from groups 4−10 and X is a chalcogenide such as S, Se, or Te), that have bandgaps ranging from ∼1.1 to 2.5 eV.[11,19] Growing consideration also has been given to the chemistry of black phosphorus (BP), whose layered polymorphic structures give this element's most thermodynamically stable allotrope a tunable direct bandgap (∼0.3 to 2.0 eV), suitable for use in optoelectronics.[19,33,66−69]

Depending on the conditions used in their synthesis (and the specific materials composition involved), monolayer (ML) sheets and flakes can be peeled from a bulk sample via mechanical exfoliation (ME). A schematic depiction of this process is given in Figure 1a, where an adhesive tape is used to peel back a ML of material for transfer to a supporting substrate. An image of a transferred MoS_2 NM is shown in Figure 1b.[70] This approach makes it possible to explore TMD and BP NM devices and there now exist many reports of high-performance optoelectronic devices[70−82] and transistors (with mobilities on the order of ∼200 $cm^2\ V^{-1}\ s^{-1}$) utilizing them as an active electrical material.[83−94] ME remains the simplest approach to obtain high quality samples, although with challenges to both yields and scaling. Specifically, fabrication methods suitable for use with BP remain an area of need even as research continues to build better understandings of its electronic and structural properties, and explores means to stabilize it against decomposition.[92,94−100]

While the simplicity of ME has yielded high-performance materials suitable for use within a laboratory setting, its utility for broad scale adoption in technology remains limited. Liquid-phase exfoliation (LPE, a process shown in Figure 1c) provides a promising alternative means of preparing high quality 2D NMs from intrinsically layered solid materials. To exfoliate thin films in this way, a solvent (or surfactant) must be able to overcome the VDW forces between the material layers and prevent aggregation of the separated sheets. With suitable choices, relatively large single sheets (such as the MoS_2 films shown in Figure 1d) can be prepared.[101] Coleman and co-workers have studied the solution phase processing of TMD materials and have identified solvent properties (e.g., surface tension of ∼40 mJ m^{-2}) that permit production of single- and few-layer sheets[101] in a manner analogous to processes used with graphene.[102,103] A number of organic solvents have been shown to be promising for exfoliation of TMD sheets that yield large area (>100 nm) flakes in useful quantities.[101,104−106] Efforts using similar solvents are being used to exfoliate BP, although with limited success in consequence of its stability.[107−111] The LPE of TMDs in aqueous media is also of significant interest, where (given water's surface tension of 72 mJ m^{-2}) the addition of surfactants is required to maintain stable dispersions. For example, Smith and co-workers were able to exfoliate thin sheets of multiple TMD materials including MoS_2, BN, WS_2, $TaSe_2$, $MoTe_2$, $MoSe_2$, and $NbSe_2$ using sodium cholate as a dispersant.[112]

Chemical intercalants can also be used. The insertion of lithium ions between adjacent TMD layers using *n*-butyl lithium[17,113,114] and sonicating either during lithium insertion[115] or after[116−119] illustrates this chemistry, yielding materials with properties useful for applications spanning from electrocatalysis to electronic/optoelectronic devices.[11,106,116,120−122] The intercalation of Li can also be driven electrochemically to accelerate its uptake.[116−118,122−124]

Direct Chemical Synthesis of 2D NMs. In concept, a direct pathway to synthesize 2D NM materials would proffer advantages over alternative methods based on either ME or LPE. A bottom-up fabrication technique of this form would require capacities to select forms of growth (specific polymorphs, etc.), support substrates, and, for full generality, the possibility of effecting physical transfers post growth. Toward this end, chemical vapor deposition (CVD) and other thermolytic processing methods have been examined as routes to NMs, both for cases based on intrinsically bulk layered structures as well for very thin layers of otherwise extended bulk solids. Examples here include the growth of TMDs as well as extreme terminations of bulk semiconductor structures such as silicene (single-layer Si) and 2D GaN.

A well-studied bottom-up synthesis is that of the CVD growth of the TMD material MoS_2.[125−136] Procedures to deposit thin layers of MoS_2 can be translated to other TMD materials (e.g., $MoSe_2$, WS_2, WSe_2, etc.)[137−144] and so well represent strategies for the broader class. The schematic in Figure 1e outlines a prototypical CVD process, one in which MoO_3 and sulfur are used as the elementary Mo and S sources, respectively. The deposition is carried out at high temperatures (650 °C) under $N_{2(g)}$ flow in order to induce the reduction of MoO_3 by the S vapor to the volatile suboxide MoO_{3-x}, which then reacts further with the S vapor on the substrate surface to form MoS_2:[125]

$$MoO_3 + x/2S \rightarrow MoO_{3-x} + x/2SO_2 \quad (1)$$

$$MoO_{3-x} + (7 - x)/2S \rightarrow MoS_2 + (3 - x)/2SO_2 \quad (2)$$

This film growth is not inherent on the supporting substrate and a seed layer (i.e., reduced graphene oxide, perylene-3,4,9,10-tetracarboxylic acid tetrapotassium salt, or perylene-3,4,9,10-tetracarboxylic dianhydride) must be used.[125] With an optimized seed layer, the dimensions of the NMs can be improved. Alternative precursors include a thin Mo film (deposited on the substrate and subsequently reacted with S vapor to produce MoS_2)[127] and $(NH_4)_2MoS_4$,[128,129] where the thermolysis reaction proceeds as follows:

$$(NH_4)_2MoS_4 + H_2 \rightarrow 2NH_3 + 2H_2S + MoS_2 \quad (3)$$

A second annealing step in the presence of S vapor at 1000 °C is required in order to increase domain sizes and improve crystallinity. There now exists a rich and growing literature discussing the growth of TMD NMs and the impacts that precursor chemistry, seed layers, substrates, and growth dynamics have on properties important for their use in electronic and optoelectronic devices.[126,130−144]

Heteroepitaxial structures of TMD and BP materials can be prepared by CVD.[145−151] Both vertical[146,149] and lateral[145,147,148,150] heterostructures have been reported with superior properties as compared to stacked NMs adhering via VDW interactions. Materials with large lattice mismatches (e.g., WS_2 and WSe_2, 4% mismatch) can be grown with lattice coherence and specific supercell dimensions.[145] Figure 1f shows an optical image and photoluminescence intensity maps of a $MoSe_2/WSe_2$ heterostructure grown in a one-pot synthesis by simply controlling the gas composition within the reaction chamber,[147] a process extendable to other MoX_2 and WX_2 heterostructures.[147,148] *In situ* growth of the TMDs provides pristine junctions between the two materials as well as allowing distinct control over domain sizes. Electrical characterization of

DOI: 10.1021/jacs.8b04225
J. Am. Chem. Soc. 2018, 140, 9001−9019

Table 1. Electronic Properties of 2D NM Materials

2D NM	Synthesis	Electron mobility ($cm^2 V^{-1} s^{-1}$)	Hole mobility ($cm^2 V^{-1} s^{-1}$)	On/Off Ratio	Reference	Comments
TMD	ME	25−30, 100−200	180*−350	10^4−10^8	83, 84, 86−89*	*NO_2 doped
TMD	CVD	0.02−80	−	10^3−10^6, 10^8*	85, 125, 127, 132, 139, 209*−213	*HfO_2 dielectric
TMD	LPE	0.117/162−195*	−	3−4	105	*corrected values
BP	ME	10	10−300; 984;* 1,350**	10^3−10^5	92,93*−96, 99, 100**	*10 layers **hBN-BP-hBN heterostructure
a-BP	CVD*	−	0.5	10^2−10^4	152,153	*CVD of red P, then converted to BP with pressure
BP	LPE	−	<50	10^3	109	
a-BP	PLD*	−	14	10^2	154	*Pulsed laser deposition
Silicene	Evap.	114	72	10	160	

the heterojunctions displays the typical rectifying behavior of well-defined p−n junctions.[147]

BP NM films can be grown on Si/SiO_2 substrates at high pressure using amorphic red phosphorus as a precursor; the electrical properties of the materials produced have been explored in model FETs.[152,153] It also has been suggested recently that the amorphous form of BP (a-BP) might be of interest for use in electronics in a manner similar to amorphous silicon, although the performance levels of FETs using it as an active semiconductor (mobilities of 14 $cm^2 V^{-1} s^{-1}$ and on/off ratio of 10^2) remain modest.[154]

Recent literature describes the chemical synthesis of single- and few-layer 2D GaN and silicene. While 2D hexagonal boron nitride (hBN) NMs have been studied extensively,[155,156] studies of other nitride materials remain limited due to their general adoption of nonlayered bulk structures. For example, wurtzite GaN is tetrahedrally coordinated and unsaturated dangling bonds significantly impact its properties at the nanoscale. A recent report describes a method to passivate these dangling bonds and grow 2D GaN films through migration-enhanced encapsulation growth (MEEG, Figure 1g).[157] Here, an epitaxial graphene layer is first formed via sublimation from a SiC(0001) substrate followed by hydrogenation (Figure 1g, steps 1 and 2). Trimethylgallium is then decomposed on the graphene/SiC(0001) surface, where gallium adatoms penetrate the graphene capping layer (steps 3−5) and then converted to GaN via ammonolysis (step 6).[157] A high-angle annular dark-field scanning transmission electron microscopy (HAADF-STEM) cross-sectional image of the encapsulated 2D film is shown in Figure 1h.

Perhaps the most interesting NMs are those composed of Si, materials we treat at some length in the sections that follow. Silicene, as a limiting case, has been treated in theoretical studies in considerable depth since the discovery of graphene.[51,158] In a manner analogous to graphene, silicene exhibits a Dirac bandstructure and as a result of its buckled structure, exhibits a discrete bandgap due to its lowered symmetry.[24,159,160] Unlike graphene, which is sp^2 hybridized, silicene exhibits a mixed sp^2-sp^3 hybridization due to its larger ionic radius,[23,161] a perturbation that drives its nonplanar structure. It is only recently that supported silicene sheets have been grown experimentally (via thermal evaporation), as shown schematically and in the microscopy images shown in Figure 1i,j, respectively.[162,163] Silicene nanoribbons form on Ag (110) surfaces,[164−167] which mediates growth via adatom diffusion along the $[\bar{1}10]$ direction of the substrate.[164] Silicene sheets grown on Ag(111) surfaces exhibit the expected buckling structure.[162,168,169] Several superstructures of silicene have also been identified whose nature depends strongly on substrate temperature and deposition rate (Figure 1j).[162,163,169] On average, single layer domains of silicene remain limited in size (ca. 100 nm^2) and are not generally amenable for release from their growth substrates;[160,162,163,168,169] growth on other substrates has been explored in this regard.[170,171]

Table 1 provides a summary of the electronic properties of 2D NMs prepared in various ways. Notable differences are clearly evidenced between ME and CVD sourced materials. A challenge for CVD-grown materials, and bottom-up growth in general, is obtaining highly crystalline sheets. Subsequent steps (e.g., thermal processing) are generally needed to improve the material's electronic properties. A further challenge is the ability to control the number of 2D layers that are deposited while maintaining electronic and optoelectronic properties superior to those obtained by exfoliation. Unquestionably, however, the sourcing of NMs directly from electronic grade wafer/bulk semiconductor sources (e.g., Si and III-V materials) remains perhaps the most attractive approach for realizing scalable approaches for applications in technology (an idea we illustrate with examples taken from the recent literature in the sections that follow).

Synthesis of Single-Crystalline NMs. The use of single-crystalline semiconductors remains a central materials requirement for high-performance electronics. The breadth of knowledge in Si processing has enabled the fabrication of new classes of devices using them in flexible and transient electronics among a range of form factors that variously exploit wafer-scale processes to extract thin films from bulk-like sources.[1,5−7,48,172] Related strategies have also been developed for use with III-V semiconductors for applications where direct bandgap materials are required. The preparation of thin single-crystalline NMs exploits approaches outlined below. These strategies employ precise top-down etching capabilities as well as epitaxially grown films that accommodate lattice mismatch in interesting ways to create novel materials sets. Recent advances in top-down approaches provide access to Si NMs on a large scale and further allow doping, as well as integration of the dielectrics (e.g., SiO_2), device components, and barriers/encapsulating structures required. Selective etching (Figure 2a−c) is commonly used to obtain Si NMs, particularly anisotropic etching,[60,173−175] which utilizes the selectivity of specific etchants toward the impacts of electronic structure on the bonding of Si atoms within specific high-symmetry, low-index crystalline planes. Close-packed {111} planes have comparatively slow etching rates, followed in order by {100} and {110} planes, which progressively etch more rapidly. These rate-structure sensitivities can be utilized to produce

DOI: 10.1021/jacs.8b04225
J. Am. Chem. Soc. 2018, 140, 9001−9019

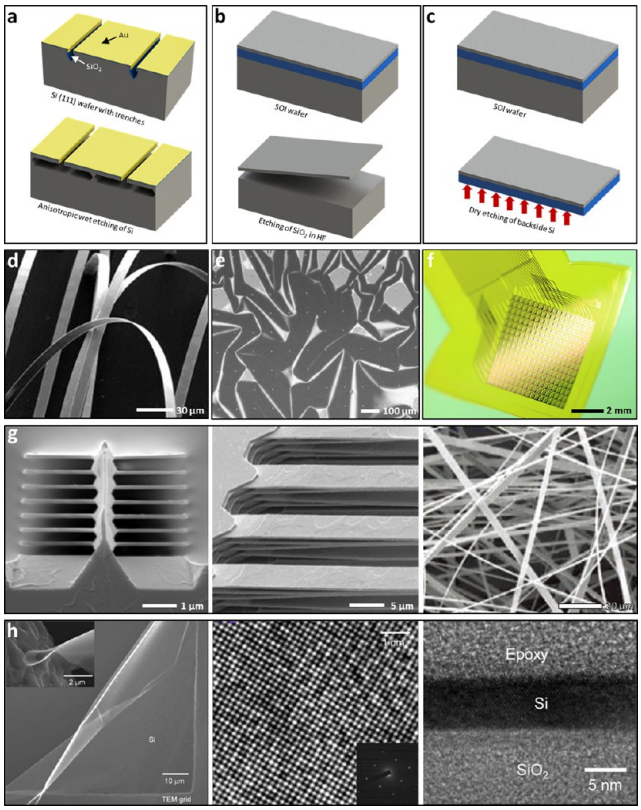

Figure 2. Silicon NM synthesis. (a–c) Schematic illustrations of fabrication processes and of Si NMs, including (a) anisotropic etching, (b) etching of the buried oxide, and (c) back etching. (d–f) Images of Si NMs prepared from (d) anisotropic etching,[173] (e) etching of the buried oxide,[1] and (f) back etching.[61] (g) SEM images of multilayer Si NMs.[60] (h) SEM and TEM images of ultrathin Si NMs.[8] Reproduced from ref 1 with permission from Springer Nature, ref 8 from ACS, ref 61 from PNAS, and ref 173 from AIP Publishing.

specific structural features depending on the orientation of the wafer.[176−180] In Figure 2a, an anisotropic etching process is illustrated in which trenches are first defined on Si (111) wafers through patterned reactive ion etching (RIE) to expose the {110} planes. Selectively patterned SiO_2 and evaporated metal passivate the top and sidewalls of Si and an anisotropic etch in KOH undercuts the Si along the ⟨110⟩ directions, thereby forming Si NMs after release. The general form of the net chemical reaction in this case is given by the following:

$$Si + 2OH^- + 2H_2O \rightarrow Si(OH)_2O_2^{2-} + 2H_2 \quad (4)$$

which is consistent with the observed production of $Si(OH)_2O_2^{2-}$ and two hydrogen molecules per Si atom.[177,181] Figure 2d shows an SEM image of released, mechanically flexible Si nanoribbons.[173] Other forms of Si NMs are also possible using a similar anisotropic etching strategy. One example generates Si NMs in multilayer stacks,[60] exploiting the rippled sidewall structure that results from a deep inductively coupled plasma (ICP) RIE in the Bosch process.[182] Angled evaporation of metals and anisotropic KOH etching of Si yield multilayer Si NMs that can be readily released or transfer printed, as shown in the left and middle frames of Figure 2g, or released in bulk quantities, as shown on the right in Figure 2g. This high-throughput processing technique efficiently utilizes a large volume of the bulk source wafer.

An alternative way of making Si NMs exploits selective etching of a buried oxide layer using a silicon-on-insulator (SOI) wafer, where a thin single-crystalline layer of Si is bonded atop a base handle wafer by a sacrificial layer of SiO_2 (Figure 2b). Hydrofluoric acid is used to etch away the buried oxide layer. The top Si device layer can then be released or transferred to another substrate. Figure 2e shows an image of a Si NM with a thickness of ∼50 nm that was so prepared.[1]

A recent development also begins with the use of SOI wafers, but replaces the wet etching of the oxide layer with dry etching of the back Si handle wafer, as in Figure 2c. Removal of the backside of the Si wafer typically involves grinding of the backside, followed by a series of RIE steps to completely remove the Si on the back side. Si NMs formed in this way keep the buried SiO_2 layer, which can serve as protective barriers for biointegrated electronic systems (*vide infra*).[61] The optical image in Figure 2f presents a Si transistor array in which the Si NMs were so encapsulated by SiO_2.

It is possible to prepare ultrathin Si NMs (1.4 to 10 nm) using cycles of thermal oxidation and etching.[8,183] This process uses similar etching strategies as for SOI wafers but first thins a portion of the top Si device layer by thermally oxidizing and subsequently etching it. This process reduces the thickness of top Si device layer to ∼16 nm. The second thinning process exploits repetitive ultraviolet-ozone (UVO) oxidation and removal of SiO_2, which controls the oxidation/etches more precisely to ∼0.74 nm of Si each cycle.[8] Figure 2h presents an SEM image (left), a high-resolution TEM image (middle), and a TEM side view (right) of an ultrathin Si NM so prepared. These NMs exhibit quantum confinement effects as well as high flexural compliance and optical transparency— distinguishing functional attributes for devices as are described below.

The release of III-V NMs is best achieved via selective etching of a buried sacrificial layer. This layer can be included in a repeated epitaxial stack[62,184] that is either lattice matched or otherwise accommodative so as to not produce defect inducing strains and selected to etch at significantly higher rates than the device layer. This allows substantial latitude for processing and fabrication steps prior to lift-off and proves most beneficial when the receiving substrate (e.g., an organic polymer) cannot accommodate the harsh processing conditions as might be required (i.e., corrosive etchants, etc.).

An example of an epitaxial stack is shown in Figure 3a, where an alternating structure of GaAs (the device layer) and AlAs (the sacrificial layer) is built up by an MOCVD process in a stack that allows the release of large quantities of GaAs NMs (Figure 3b)[184] as well as thin, flexible devices (Figure 3c).[185] This approach, called epitaxial lift-off, has been developed extensively[62,184,186−190] and has greatly reduced the cost of GaAs and other III-V semiconductors, enabling their widespread use as high efficiency electronic and optoelectronic devices. Epitaxial lift-off encompasses the single-crystalline quality of an epitaxially grown film as well as the ability to reuse the support wafer for the growth of new epilayers. To etch $Al_xGa_{1-x}As$, hydrofluoric acid is used due to the selectivity afforded by an etch rate that increases markedly with the aluminum fraction. For example, etch rates of $Al_xGa_{1-x}As$ ($x > 0.6$) are $>10^6$ times faster than that of GaAs in hydrofluoric acid.[190] Typically, AlAs is used as a sacrificial layer as it demonstrates the highest selectivity for the system. The chemical reaction between aqueous HF and AlAs produces a complicated speciation of products that includes aluminum

DOI: 10.1021/jacs.8b04225
J. Am. Chem. Soc. 2018, 140, 9001−9019

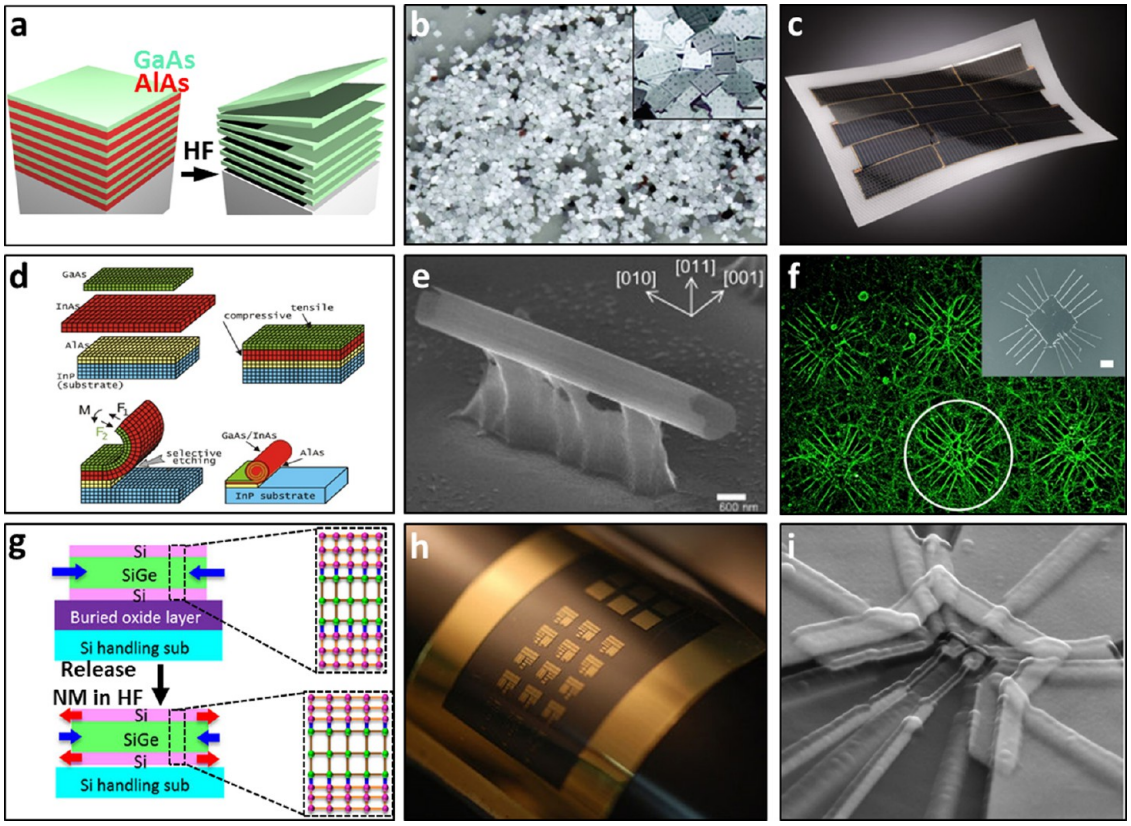

Figure 3. Synthesis of epitaxial NMs. (a) GaAs epitaxial structure. (b) Multiple GaAs PV devices prepared from epitaxial lift-off. Scale bar (inset), 200 μm.[184] (c) Flexible GaAs PV array.[185] (d) Schematic of NM self-rolling[16] and (e) InAs/GaAs NM self-rolled tube.[194] (f) Si/SiGe NM self-rolled tubes directing cell growth. Scale bar, 100 μm.[41] (g) Schematic of strained SiGe NM preparation and (h) image of a strained SiGe transistor array.[197] (i) SEM of a double QD structure on a Si/SiGe NM.[32] Reproduced from ref 16, 32 with permission from IOP Publishing, ref 41 from ACS, ref 184, 197 from Springer Nature, ref 185 from Cambridge University Press, and ref 194 from Elsevier.

fluoride, arsine gas, and oxygenated species (AsO^+, $AsOH^-$, and AsO_2^+). The overall reaction (which neglects some of this complexity) can be written as

$$AlAs + 3HF + 6H_2O \rightarrow$$
$$AsH_3 + [AlF_n\cdot(H_2O)_{6-n}]^{(3-n)+} + (3-n)F^- + nH_2O \quad (5)$$

where n = 0, 1, 2, 3.[190,191] Even though the etch rates are very fast, mass transfer effects can limit the etching processes as the sacrificial layers are very thin and species must diffuse in and out of the crevices created by the dissolution of material. To combat this, techniques have been developed that slowly peel back the device layer as etching proceeds in order to better expose the active area of the sacrificial layer,[188,189] as well as to infuse gases such as oxygen to inhibit As deposition (from AsH_3, which acts as a barrier for further etching).[191,192]

Other compound semiconductors can use epitaxial lift-off processes to fabricate NMs. For example, AlGaSb can be used as a sacrificial layer in the fabrication of InAs or InGaSb NMs.[30,31,63] The scope of the inorganic NMs that can be so fabricated is quite broad, with many choices for the sacrificial layers, etchants, and strategies to mitigate lattice strains that would otherwise induce defects.

Sacrificial layers are typically chosen to minimize strains within the device layer. Such strain can be utilized, however, to induce shape transformations. In cases where the NM materials are grown on substrates with significantly larger (or smaller) lattice constants, the released NMs can curl up into precise tubular shapes.[15,16] This concept is shown schematically in Figure 3d. The InAs epilayer shown has a larger lattice constant than the base substrate and is compressively strained; the top GaAs epilayer is under tensile strain.[16] Upon selective etching of the AlAs sacrificial layer, the InAs layer tends to expand while the GaAs layer compresses. These opposing forces, F_1 and F_2, result in a net momentum, M, that induces the NM to roll up.[16,193] This makes it possible to prepare tubes, rings, coils, and a host of other geometries. An example of a InGaAs/GaAs tube is shown in Figure 3e, balancing on a thin sacrificial layer of $Al_{0.6}Ga_{0.4}As$.[194] Depending on the orientation of the lithographically patterned stripes, the NMs can be rolled into tubes, flowers, and coils.[194]

In addition to III-V materials, strain-driven assembly is applicable to other lattice mismatched films such as Si epitaxially grown on SiGe-on-insulator (SGOI) wafers.[195] The applications for Si-based materials are quite different and can include biological studies, as shown in Figure 3f.[41] Here, Si/SiGe nanotubes are utilized as a biologically viable substrate providing cues for outgrowth of primary cortical neurons and selectively allowing single axon growth inside of the tubes when tube diameters are on the order of 4 μm. The tube diameter can be accurately controlled via the Ge concentration in the $Si_{1-x}Ge_x$ alloy and the thicknesses of the Si and SiGe layers. Using semiconductor structures as 3D scaffolds for tissue growth provides a general strategy for defining neuronal networks that can also be electrically probed.[41,196]

DOI: 10.1021/jacs.8b04225
J. Am. Chem. Soc. 2018, 140, 9001−9019

The strains induced by lattice mismatch can be utilized to prepare strained-Si and -SiGe NMs for applications in quantum electronics and fast flexible electronics. The application of strain is known to change the electronic band structure of materials and specifically Si shows an increase in carrier mobility with strain.[13,197,198] The fabrication of strained-Si is limited, however, by techniques that grow Si on compositionally graded $Si_{1-x}Ge_x$ substrates. These films tend to exhibit misfit dislocations and lack the structural uniformity imperative for quantum electronics.[13,198] Figure 3g illustrates an alternative technique in which Si/SiGe/Si NM trilayers are used to fabricate strained-Si NMs and Si/SiGe/Si quantum well structures.[197] A SiGe layer is epitaxially grown on an SOI wafer and a Si capping layer is then epitaxially grown on top. The lattice mismatch induces a compressive strain in the SiGe layer, which is then partially released via strain sharing with the Si layers, now tensilely strained after lift-off in hydrofluoric acid. Using this strategy, Zhou and co-workers fabricated a flexible thin film transistor (TFT, Figure 3h) demonstrating a 47.3% enhancement in effective mobility.[197] An alternative structure, SiGe/Si/SiGe, can be fabricated where a strained-Si quantum well is grown on an elastically relaxed SiGe NM,[32] providing a gate-defined double quantum dot in the Si/SiGe NM (Figure 3i) that can be tuned by a magnetic field.[32] Quantum-well infrared emitters and photodetectors can be fabricated similarly.[14,199]

The most promising routes for preparation of NM materials are high-throughput techniques that preserve the high electronic quality afforded by their bulk counterparts. The approaches outlined above take on these demanding objectives. The progress made includes next-generation devices that enable high performance in regimes that have classically been difficult to realize. Exemplary demonstrations in these fields for 2D-, Si-, and epitaxial-NMs are discussed below.

3. ELECTRONIC AND OPTOELECTRONIC NANOMEMBRANE DEVICE APPLICATIONS

2D NM Transistors and Optoelectronic Devices. When bulk materials are thinned to atomic dimensions, quantum confinement effects can be exploited to provide new forms of functionality for electronic and optoelectronic devices. For example, TMDs can have an indirect bandgap as bulk materials (e.g., MoS_2 and WS_2), yet exhibit a direct bandgap below a specific number of layers.[11,17] This transition engenders an enhanced photoluminescence that can be utilized in unique ways, including as optoelectronic materials for light-emitting diodes (LEDs). Theoretical investigations also suggest that 2D materials would be useful in spintronic and valleytronic technologies due to strong spin−orbit and spin−valley coupling in silicene and group VI TMDs, respectively.[17,38,200] Single-layer BP has been shown to exhibit anisotropic electrical behaviors as a result of the unique features of its crystalline structure.[22,98,201−205] Such properties suggest prospects for electronic devices employing 2D materials with useful features that would not be possible with bulk materials.

One of the most persuasive arguments for continued efforts in research of 2D materials is provided by the transistor. In accordance with Moore's Law, technology has minimized the critical feature sizes in transistors to deliver faster and more efficient devices. In moving forward, short-channel effects (such as current leakage between the source and drain) become extremely problematic. Field-effect transistors (FETs) made from 2D materials (where electrons are strongly confined in the atomic layer) are less significantly impacted. Ideally, 2D channel materials would be compatible with complementary metal oxide semiconductor (CMOS) processing and therefore, silicene has been imagined as the quintessential 2D channel material. Initially, most research on this material was theoretical[24,38,161,164,165,200,206] but recently Tao and co-workers have reported a method to delaminate and encapsulate a silicene NM for subsequent integration into a working FET (Figure 4a).[160] This device

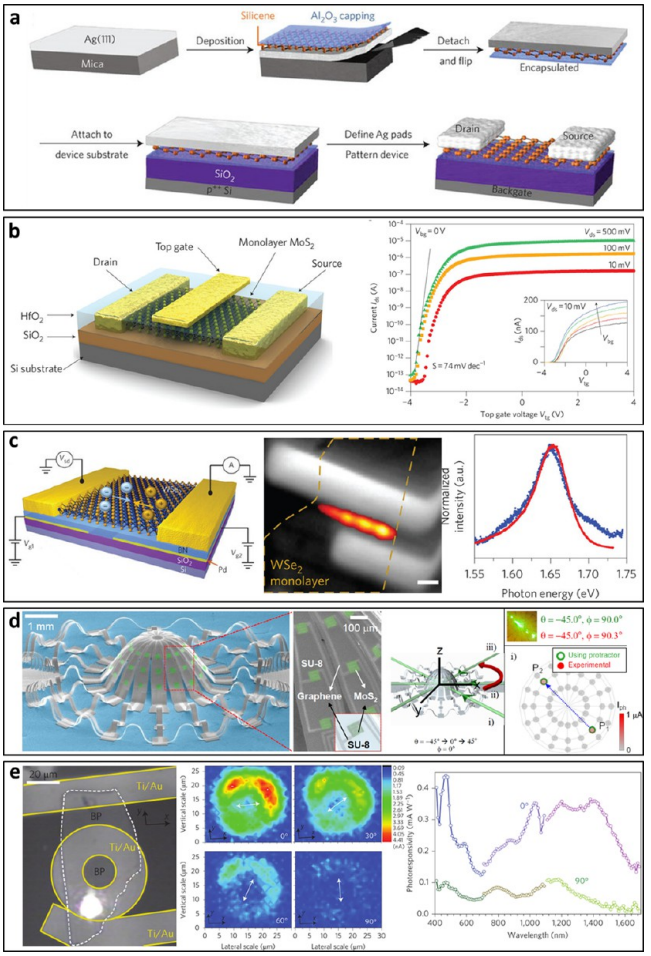

Figure 4. 2D NM electronic and optoelectronic devices. (a) Schematic of the method to prepare a silicene FET.[160] (b) Schematic of a MoS_2 FET with HfO_2 dielectric layer (left) and its transfer characteristics (right).[83] (c) Schematic of a gated WSe_2 LED (left), electroluminescence image (middle, scale bar, 2 μm) and spectrum (right).[71] (d) SEM (left) of a 3D SU-8 structure (dark gray) with MoS_2 photodetectors (green) interconnected with graphene (light gray) and its angular photodetection as compared to a protractor (right).[225] (e) BP photodiode with a ring electrode (left), photocurrent microscopy images at 0°, 30°, 60°, and 90° polarization angles (middle), and photoresponsivity at 0° and 90° (right).[69] Reproduced from ref 69, 71, 83, 160, 225 with permission from Springer Nature.

displayed a current on/off ratio of only 10, but average electron and hole mobilities of 114 and 72 cm^2 V^{-1} s^{-1}, respectively. The low current on/off ratio is an indication of the small bandgap of silicene (~210 meV).[160] This form of silicene was used to fabricate a self-switching diode (SSD),[207] permitting modulation of conductance.

FETs based on semiconducting TMD materials have witnessed marked improvements in carrier mobilities in part

DOI: 10.1021/jacs.8b04225
J. Am. Chem. Soc. 2018, 140, 9001−9019

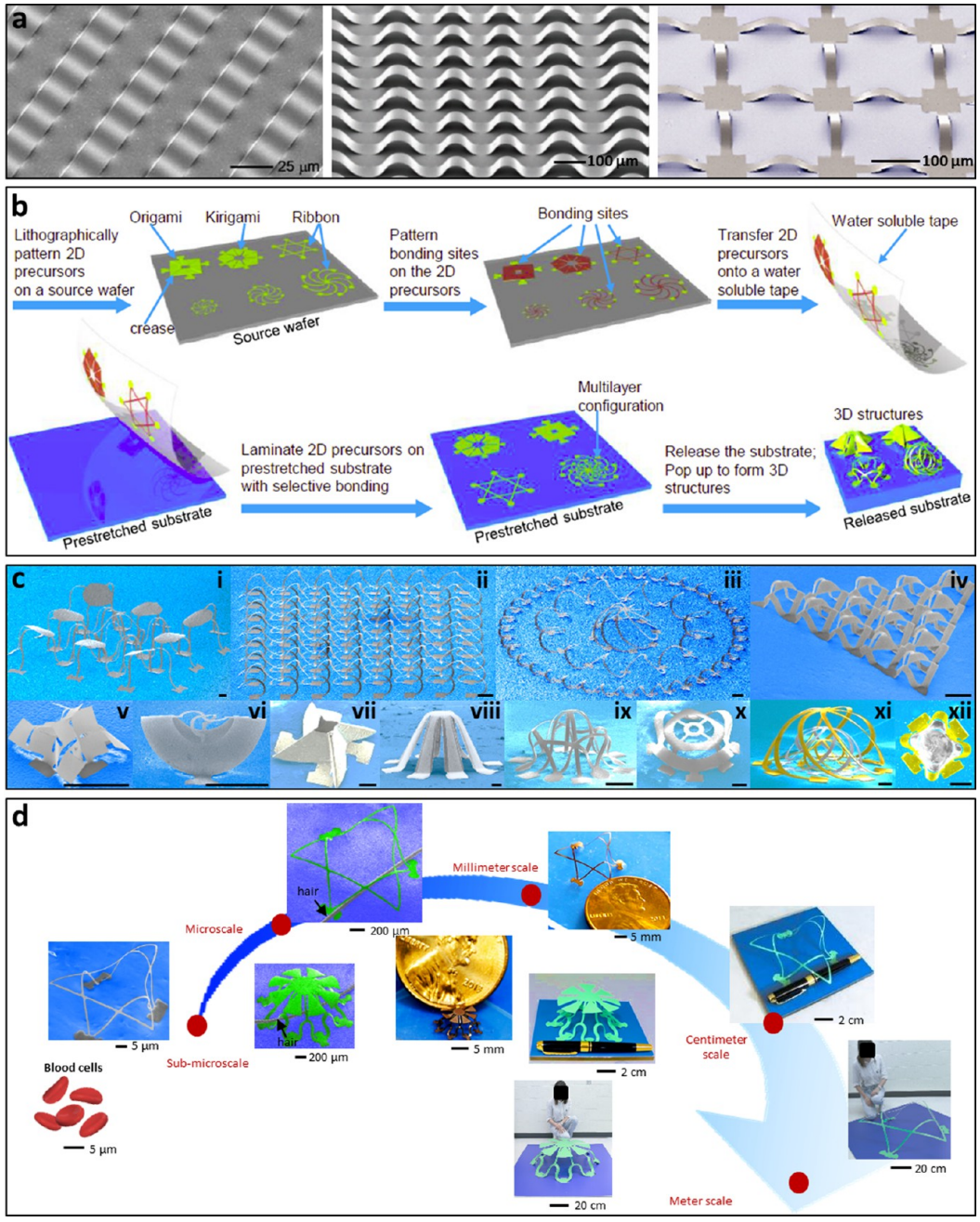

Figure 5. Assembly of Si NMs. (a) SEM images of Si NM assembled into 3D shapes, involving an array of wavy Si nanoribbons (left),[64] controlled buckling of Si nanoribbons (middle),[238] and arc-shaped open-mesh structures buckled in two dimension (right).[239] (b) Schematic illustration of the deterministic assembly of 3D mesostructures.[50] (c) SEM images of representative 3D mesostructures made of Si. Scale bars, 200 μm.[65,240−242] (d) Assembled 3D structures that span from submicron scale to meter scale.[48] Reproduced from ref 64, 240, 242 with permission from AAAS, ref 48 from Elsevier, ref 50, 238 from Springer Nature, ref 65 from John Wiley & Sons, and ref 239, 241 from PNAS.

through the incorporation of high-κ gate dielectric materials (e.g., HfO_2). A schematic depiction of an exemplary device and its transfer characteristics are shown in Figure 4b.[83] The measured mobilities surpass prior limiting values for MoS_2 FETs (0.1−10 $cm^2\ V^{-1}\ s^{-1}$), reaching 217 $cm^2\ V^{-1}\ s^{-1}$.[83,158] This strategy was used to fabricate four different integrated logic circuits including an inverter, a NAND gate, a static random access memory (SRAM) cell, and a five-stage ring oscillator,[208] results suggesting a very promising future for TMD and other 2D NM-based devices, if challenges to device performance and stability can be solved, including: contact resistance;[84,89,92,209] encapsulation/stabilization against oxidation;[84,92,94−96,99,100] doping;[11,85−89,92,94,96,99,139,210] and improved carrier mobilities.[19,93,125,127,132,211−214]

For 2D materials possessing direct bandgaps, use as an active material for LEDs with large photo- and electroluminescence intensities has been explored. BP films have a direct bandgap (0.3 eV) suitable for near-infrared (NIR) and infrared (IR) detection and emission.[19] The high absorptivity values for 2D materials (e.g., $>10^6$ for TMD materials)[215] further provides interesting prospects for thin film photovoltaic devices.

For most optoelectronic devices, it is beneficial to create a $p-n$ junction that effectively separates electron−hole pairs. Photovoltaic and electroluminescent efficiencies have been

DOI: 10.1021/jacs.8b04225
J. Am. Chem. Soc. 2018, 140, 9001−9019

shown to greatly benefit from this.[72,82,216] Schottky barriers at the semiconductor/metal interface can be exploited to separate e−h pairs in consequence of the built-in potential present at the junction.[80,217,218] Additionally, electrostatic doping via an applied voltage at the gate electrode using either a metal[71,73,81,82,219−221] or graphene[76,222,223] electrode, or more recently a triboelectric nanogenerator[224] can be utilized for that purpose. An example of such an electrostatically doped device using a Pd electrode is shown in Figure 4c. Here, the back gates are separated from the TMD material, WSe_2, by hBN.[71] When the Pd back gates are biased to form the $p-n$ junction, bright electroluminescence is observed (Figure 4c, middle) at a low current of only 5 nA. The spectrum on the right in Figure 4c shows this electroluminescence in blue along with the corresponding photoluminescence in red. The similarity in each spectrum suggests that the electroluminescence is derived from similar mechanisms as photoluminescence in which direct-gap excitons recombine radiatively.[72,77,78] This is an important observation as photoluminescence experiments have confirmed that excitons form in the ±K valleys, suggesting that excitons from electroluminescence do so as well. TMDs are unique in that they have two inequivalent momentum valleys, +K and −K, that are required to have opposite spin due to time-reversal symmetry. This enables spin-valley coupling, in which spin- and valley-LEDs might produce polarized emission from spin-polarized injection via ferromagnetic contacts.[17,71]

Promising schemes for achieving $p-n$ junctions in TMDs also include utilizing ionic liquids to replace the gate dielectric in WS_2 FETs,[78] plasma-doping MoS_2 flakes,[74] and band-structure engineering.[77] Heterojunctions between 2D materials can also be utilized to create $p-n$ junctions for optoelectronic devices. BP, for example, is a predominately p-type material with exceptional hole mobilities, and its integration with MoS_2 provides a gate-tunable $p-n$ diode[67] with promise for high efficiency thin film solar cells.[68]

Figure 4d shows an extension of 2D optoelectronic devices, one exploiting a strain-driven 3D assembly process (detailed below).[225] A photoresist, SU-8, acts as the scaffold material supporting out-of-plane bending, enabling affixed MoS_2 photodetectors to be driven upward for three-dimensional photodetection. This structure is shown on the left in Figure 4d, with an example of its angular detection on the right. The response of the photodetector array is unique in its ability to detect light at two locations, the entry (P_1) and exit (P_2), due to its optical transparency. This allows for detection of both the position and intensity of the incident light, as demonstrated on the right in Figure 4d.[225] Related designs for MoS_2−graphene heterostructures offer optical signal detection as well as programmed electrical stimulation capabilities for use in soft retinal prosthesis.[226]

The optical anisotropy of BP gives rise to linear dichroism within the material[204] and because of this phenomenon, polarization-dependent photodetectors in the IR region have been explored. Figure 4e shows a BP photodetector[69] using a ring-shaped metal contact to suppress influences of the metal electrode edge on specific polarizations, allowing the photogenerated hot carriers to be collected isotropically. As seen in the photocurrent microscopy images in the middle of Figure 4e, the photoresponsivity exhibits distinct polarization sensitivity, and the spectra on the right in Figure 4e demonstrate consistently higher (~3.5×) photoresponsivity for light polarized at 0° (the armchair direction) than light polarized at 90° (the zigzag direction).

The intrinsic electrical anisotropy of BP has also been explored in 2D-NM junctions in terms of thermoelectric properties,[202,205] although the figures of merit (ZT) measured to date are modest.[227−230]

Constructs of Single-Crystalline NMs That Enable Transient, Flexible, and Other Novel Applications. The quality of many 2D materials remains a major challenge in research. For established materials, such as Si and various epitaxially grown semiconductor materials, quality is not an issue as they are derived from electronic grade, single-crystalline source wafers. Here, we discuss new approaches to 3D device form factors, micro- and macro-scale buckled Si structures, and Si NMs as employed in so-called transient electronics for biological/biomedical applications. As direct bandgap materials are better suited for optoelectronic devices, epitaxial and III-V materials are typically utilized for these constructs. The cost of these materials can be greatly mitigated using the NM fabrication procedures discussed above, particularly epitaxial lift-off conjoined with transfer printing. The capabilities of transfer printing are reviewed elsewhere,[231−237] but these methodologies allow the preparation of complex integrated systems from device quality single-crystalline semiconductors on substrates that allow otherwise difficult to realize attributes of performance (e.g., flexible and transient electronics). We describe exemplary integrated devices in the sections that follow.

The 3D assembly of Si NMs exploits interactions between itself and a stretchable elastomer. Here, Si NMs are transferred to a prestretched elastomer,[64] where release of the prestrain drives a predetermined assembly of what can be highly complex 3D shapes. The most elementary case is shown on the left in Figure 5a. These geometries can be slightly altered by adjusting the thickness of the Si NM, changing the amplitude and wavelength of the wavy structure.

A similar approach uses lithography to add complexity in which adhesion sites are selectively defined on a prestretched silicone elastomer, enabling strategic control over the local displacements of Si NMs.[238] Selective UVO treatment of the silicone elastomer defines adhesion sites that form strong bonds to the Si ribbon. Upon release of the prestrain, areas of the Si NMs in contact with the patterned adhesion sites are tethered to the elastomer while other weakly bonded areas delaminate to adopt deterministic forms of out-of-plane bending (Figure 5a, middle). These geometries are accomplished via uniaxial prestrain, but by incorporating biaxial prestrains in the silicone elastomer the attainable geometries are expanded to arc-shaped open-mesh structures (Figure 5a, right).[49,239]

Compelling opportunities lie in the deterministic assembly of Si NMs into complex, programmable 3D shapes, including ones inspired by ubiquitous 3D mesostructures found in biology. Extended mechanically guided 3D assembly provides possibilities to access such diverse geometries including open filamentary frameworks, mixed structures of membranes/filaments, folded constructs, and overlapping, nested and entangled networks.[48,50,65,240−242] As shown in Figure 5b, the process begins with patterning 2D precursors of Si NMs, or other materials, using lithographic techniques. A second photolithography step defines bonding sites on the 2D precursors rather than on the elastomer. The preforms are then transfer printed onto a carrier (a water-soluble tape) and

DOI: 10.1021/jacs.8b04225
J. Am. Chem. Soc. 2018, 140, 9001−9019

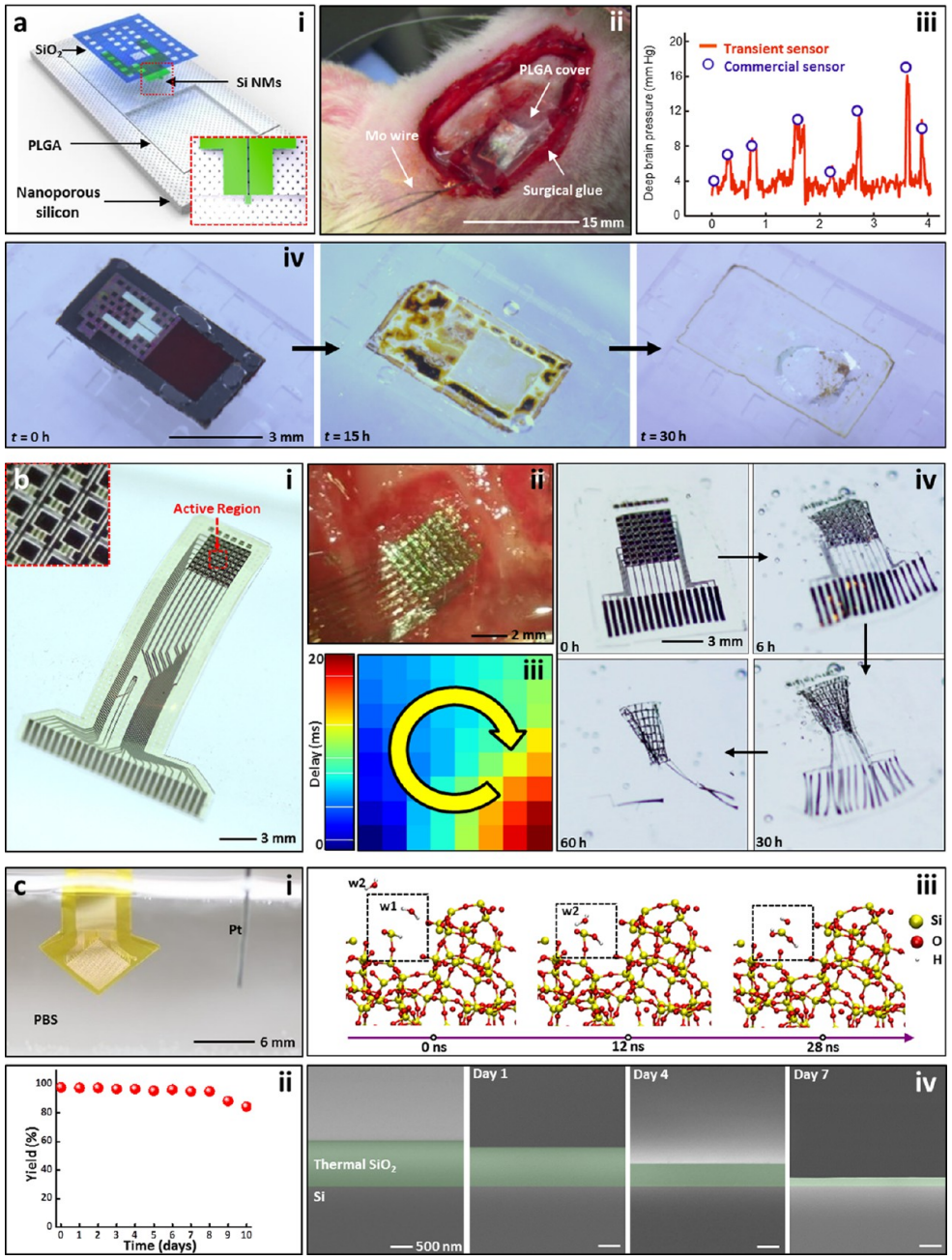

Figure 6. Bioresorbable electronics based on Si NMs. (a) i. Schematic of a pressure sensor. ii. Optical image of the sensor implanted in a rat. iii. Measurement of pressure in the brain. iv. Optical images of the sensor after immersion in aqueous buffer solution.[247] (b) Images of an actively multiplexed array before (i) and after (ii) implantation. iii. Representative delay map for the epileptic spike activity. iv. Optical images of the device after immersion in aqueous buffer solution.[248] (c) i. Image of flexible Si electronics with a SiO_2 biofluid barrier. ii. Immersion test of the encapsulation at 70 °C. iii. Molecular dynamics simulation of the hydrolysis of SiO_2. iv. SEM images of SiO_2 when immersed at 96 °C in PBS.[61] Reproduced from ref 247, 248 with permission from Springer Nature, and ref 61 from PNAS.

finally onto a prestretched silicone elastomer. In this case, releasing the prestrain in the elastomer leads to large compressive forces on the 2D precursors, delaminating and deforming the regions with a smaller work of adhesion into an explicit design-directed 3D architecture.

Representative examples of open filamentary frameworks of Si include a mixed array of tables and tents, a network of double floor helices, and circular filamentary serpentines with radially oriented ribbons, as shown in Figure 5c.i–iii.[240] Thin filaments can also be merged with larger membrane segments to form the complex structures shown in Figure 5c.iv–vi.[241] Other examples shown in the figure incorporate folded constructs of Si (Figure 5c.vii,viii),[65] overlapping and nested networks of Si (Figure 5c.ix,x),[242] and integration of assembled Si mesostructures (colorized in gray) with other materials such as a photodefinable epoxy (SU-8, colorized in yellow), as shown in Figure 5c.xi,xii.[242]

One key advantage of this deterministic assembly approach is its compatibility with conventional 2D manufacturing techniques, enabling 3D structures with many different scales (Figure 5d). The smallest case exploits Si NMs (100 nm thick) patterned through deep-UV photolithography with feature

DOI: 10.1021/jacs.8b04225
J. Am. Chem. Soc. 2018, 140, 9001–9019

sizes around 800 nm to generate a 3D starfish-like structure at the submicron scale, a size that is comparable to human red blood cells. Thin film materials beyond Si NMs are also possible using 2D manufacturing techniques. Examples include 3D structures of polyimide, bilayers of copper and polyimide, polyester, and polyvinyl chloride films that span orders of magnitude in size dependent on the chosen materials set.[48,65] Demonstrated applications of these NMs in 3D formats range from multidirectional optoelectronic devices,[225,243] to scaffolds for cells/tissue engineering,[196,244] micro/nanoscale robotics,[244] stretchable electronics,[245] and morphable electronics.[246]

In addition to flexibility, Si NMs enable rapid time scales for dissolution in water and aqueous biofluids. Controlling the temperature, pH, ionic contents, and dopant type/level of the Si can further adjust the dissolution rate.[7] In combination with other biodegradable materials (e.g., Mo electrodes, MgO dielectric layers, etc.), it is possible to construct full bioresorbable electronic systems.[6,247] The oxidative/hydrolytic degradation mechanisms of these materials can be explained using the equations below:

$$Si + 4H_2O \rightarrow Si(OH)_4 + 2H_2 \quad (7)$$

$$2Mo + 2H_2O + 3O_2 \rightarrow 2H_2MoO_4 \quad (8)$$

$$SiO_2 + 2H_2O \rightarrow Si(OH)_4 \quad (9)$$

$$MgO + H_2O \rightarrow Mg(OH)_2 \quad (10)$$

A recent example of this type of transient electronic device is the bioresorbable Si NM pressure sensor shown in Figure 6a.[247] The device consists of a Si NM utilized as a piezoresistive strain gauge, a nanoporous Si or Mg bioresorbable substrate with an air cavity sealed by poly(lactic-*co*-glycolic acid) (PLGA), and a layer of SiO_2 for encapsulation (Figure 6a.i). A change in the external pressure deflects the membrane which is read as a change in resistance. Implanted into the brain of a rat enables pressure to be monitored via controlled penetration of the device (Figure 6a.ii). Figure 6a.iii compares data from this bioresorbable sensor to a commercial pressure sensor showing the consistency and accuracy of the Si NM device. Additionally, the frames in Figure 6a.iv show the progression of an accelerated oxidative hydrolysis process for a device immersed in a pH 12 buffer solution at room temperature. Under these conditions, the Si NM and SiO_2 both dissolve in the solution within 15 h, leaving a nanoporous Si substrate that completely dissolves within 30 h.

Figure 6b highlights another example of a transient device that exploits Si NMs for an active multiplexed sensor array.[248] The Si NMs serve as the active material for an 8 × 8 transistor array, as shown in Figure 6b.i. Implanting the device into the brain of a rat allows *in vivo* microscale electrocorticography measurements (Figure 6b.ii). The relative delay map in Figure 6b.iii demonstrates a clockwise spiral during an induced seizure. Similar to the Si NM pressure sensor above, this actively multiplexed transistor array is also dissolvable *in vivo*. Under simulated conditions (i.e., aqueous buffer solution at pH 12 and 37 °C), the Si NM (300 nm thick), as well as other bioresorbable circuitry materials such as SiO_2, Si_3N_4, Mo, and PLGA, dissolve gradually (Figure 6b.iv) and (under more medically relevant conditions) completely disappear in a biofluid medium after 6 months.

Transient electronics with complex, state-of-the-art, ultrathin Si CMOS devices are also possible through release and transfer printing of foundry-produced components, including a CMOS inverter, digital logic gates, and analog amplifiers.[249,250]

Thermally grown SiO_2 does not dissolve as quickly as the Si NM and circuitry components mentioned above, and as such SiO_2 can be used as a biofluid barrier to not only prevent Si NM electronic devices from dissolving, but also to effectively avoid penetration of biofluids into the implanted devices, making these devices suitable for potential applications in long-term electrophysiology studies.[251] Simulation results show that thermally grown SiO_2 has the capability to serve as a robust barrier for over 70 years when immersed under biological conditions (i.e., pH 7.4 and 37 °C).[61] Figure 6c.i shows an array of Si transistors on a polyimide substrate encapsulated with thermally grown SiO_2 and Figure 6c.ii shows the excellent yield (defined as the number of working transistors divided by the total number of transistors) after extended immersion in a PBS buffer at 70 °C. Molecular dynamics simulations reveal important features of the dissolution chemistry (Figure 6c.iii). The steps include: a water molecule, w1, adsorbing and reacting at a −OSiH− site on the surface to hydroxylate the Si atom, forming H_2 in the process; a second water molecule, w2, further reacting with the −OSiOH− group; and the soluble $Si(OH)_2^{2+}$ complex desorbing to form silicic acid, $Si(OH)_4$, in solution. Slow dissolution processes are vital for high quality electrical performance over time scales of days and lifetimes can be predicted using thermally accelerated tests of the dissolution rate (i.e., at 96 °C). The reduction in the thickness of a thermal oxide from 0 to 7 days in such a test is evidenced in the SEM images presented in Figure 6c.iv. The data show that the initial oxide thickness is linearly correlated with lifetime measurements of the Si NM array.

Epitaxial NMs for High-Performance Optoelectronic Devices. Optoelectronic devices are enabled by transfer printing direct bandgap III-V materials. Figure 7a shows an example of such device technologies. Ultrathin AlInGaP LED structures are epitaxially grown on a GaAs substrate with an AlAs sacrificial layer and are released via an etch in hydrofluoric acid.[29] The AlInGaP LEDs are then transfer printed onto a substrate such as glass or a polymer. The example shown in Figure 7a was generated using methods analogous to those used to fabricate the buckled Si structures shown in Figure 6a. When the prestrain of the PDMS substrate is released, the metal interconnects distribute the strain within a wavy structure as is shown in the figure, with negligible impacts on the emission characteristics of the LED from the flat state (~0.3 nm for a 24% induced strain).[29] This work, among others,[28,243,252−254] illustrates the considerable potential of transfer printing in the fabrication of 3D device form factors.

The thinness of NM materials makes them ideal for applications that exploit features other than capacities for flexure as well. Notable examples are illustrated in recently reported designs for applications in photovoltaics.[62,174,175,184,255−262] For materials with high optical absorptivity, such as is the case for direct band gap III-V semiconductors, thin devices can reduce costs and improve commercial viability without compromising power conversion efficiencies. There has been extensive work directed toward improving light management in these thin solar cells, with promising potential for future developments in technology.[184,255,257,261−266] Such structures can also be shaped to adopt curvilinear forms[257] to improve capacities for light

DOI: 10.1021/jacs.8b04225
J. Am. Chem. Soc. 2018, 140, 9001−9019

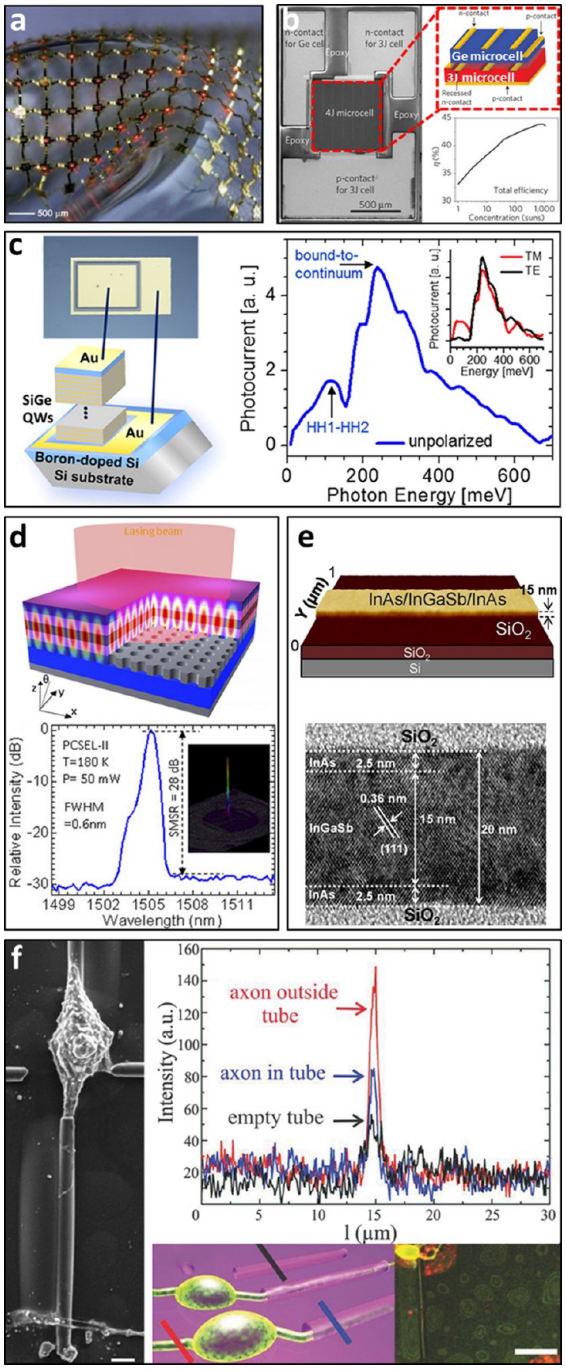

Figure 7. Epitaxial optoelectronic devices. (a) Array of AlInGaP LEDs.[29] (b) Image of 4J microcell, (left) schematic (top right), and its efficiency (bottom right).[260] (c) Strained SiGe QWIP (left) and its response (right).[199] (d) InGaAsP quantum well on a Si photonic crystal cavity (top) and its lasing output at 180 K (bottom).[272] (e) AFM (top) and TEM (bottom) of a InGaSb NM on Si.[31] (f) SEM of neurite growth on InAlGaAs/GaAs NM tubes (left, scale bar, 1 μm), intensity line plot (top right) of growth shown schematically (bottom left) and in the confocal image (bottom right, scale bar, 20 μm).[276] Reproduced from ref 29 with permission from AAAS, ref 31, 199 from ACS, ref 260, 272 from Springer Nature, and ref 276 from John Wiley & Sons.

management[264] and extend the capabilities of light-concentrating photovoltaics (CPV).[260,265,267]

Multijunction (MJ) solar cells have provided the highest efficiencies for solar energy conversion with record monolithic four-junction cells (4J) achieving power conversion efficiencies (PCEs) of 34.4% at 1 sun irradiance.[260] In principle, monolithic MJ cells can be extended to include additional band gaps to better utilize the solar spectrum and enhance performance through the minimization of thermalization losses.[268,269] In practice, however, MJ cells are burdened by difficulties beyond those of epitaxy:[268,269] most notably, current matching limitations that make integration of solar cells that absorb different parts of the solar spectrum difficult due to their varying current outputs. Mechanical stacking of NM-PV cells provides a means to overcome this difficulty, as recently demonstrated in a study of the fabrication of 4-terminal 4J microcells by stacking three junction (3J) cells atop supporting Ge base cells through the use of As_2Se_3 as the interface between them (Figure 7b).[260] The Ge cell improves the efficiency from 33.2% to 33.9% under 1 sun and further improves efficiency from 42.1% to 43.9% under ~1000 suns (Figure 7b, right). Utilizing advanced designs for concentration optics,[260] the addition of broadband, angle and polarization insensitive antireflection coatings (ARCs) via a solution based assembly process[270] provides even greater enhancements of performance and establishes a viable approach to constructing currently unrealized 5J and 6J cell designs.

In addition to III-V epitaxially grown structures, Si/SiGe and Ge NMs also find application in optoelectronics, particularly for use in the infrared.[14,35,199,271] The fabrication processes described above can be utilized here to prepare Si/SiGe heterostructures without generating misfit dislocations that limit high-performance capabilities. Figure 7c shows an example of a Si/SiGe quantum well heterostructure that exhibits intersubband transitions in the infrared.[199] A Si/SiGe NM stack is epitaxially grown on an SOI wafer and subsequently released and transferred onto a *p*-doped Si substrate. This device utilizes elastically relaxed Si/SiGe NMs to epitaxially grow multiple Si/SiGe layers, whereas heterostructures grown on traditional substrates are limited as to the number of layers due to the defects that are induced by inelastic strain relaxation. The Si/SiGe quantum-well infrared photodetector (QWIP) in Figure 7c displays two characteristic peaks, as shown on the right in Figure 7c. These peaks are associated with the intersubband transition and a bound-to-continuum transition in which the intersubband transition (i.e., ground-state subband to first excited-state subband, HH1-HH2) can only couple to TM-polarized light as designated by the polarization selection rules for such absorption. This can be seen in the inset of the spectrum in Figure 7c, where the HH1−HH2 peak disappears under TE-polarized irradiance. The resulting device exhibits a responsivity at 80 K of 73 mA W^{-1}, over twice the responsivity of a device epitaxially grown and uncompensated for the lattice mismatch strain.[199]

One interesting application of epitaxial III-V NMs is found in their integration onto Si devices.[30,31,63,256,272,273] The heterogeneous integration of compound semiconductors can benefit Si-based lasers, as their direct bandgap provides a route to higher achievable efficiencies. For example, InGaAsP was utilized as the active region in a photonic crystal bandedge laser (Figure 7d), where an InGaAsP multiquantum well NM was transfer printed onto a Si photonic crystal cavity.[272] Here, two photonic crystal surface-emitting lasers (PCSELs) were fabricated, optimized for operation at 25 and 180 K. Their operation displayed single mode lasing with spectral linewidths of 0.7 and 0.6 nm above the threshold pumping power, respectively (Figure 7d, bottom).[272]

DOI: 10.1021/jacs.8b04225
J. Am. Chem. Soc. 2018, 140, 9001−9019

The use of epitaxial NMs III-V materials can improve Si-based transistors through their use as high mobility channel materials to reduce operating voltages; the large lattice mismatch, however, has prevented their integration. NMs circumvent this issue and provide a direct means for their integration within Si devices. InGaSb and InAs NMs, for example, have been transfer printed onto Si/SiO_2 substrates for use as channel materials in a *p*-metal-oxide-semiconductor field-effect transistors (*p*-MOSFETs) and *n*-MOSFETs, respectively.[30,31] A schematic of such a design is shown in Figure 7e where a 20 nm thick InAs/InGaSb/InAs NM forms the active channel material of a *p*-type FET.[31] The TEM image at the bottom of Figure 7e shows the single-crystalline quality of the printed NM retained upon transfer. This device demonstrates a high hole mobility of 820 $cm^2\ V^{-1}\ s^{-1}$, comparable to that of strained Ge NM *p*-FETs[274] and strained buried InGaSb NM *p*-FETs,[275] which both have hole mobilities of around 1000 $cm^2\ V^{-1}\ s^{-1}$. The hole mobility for this device is also ~5× higher than that of conventional Si *p*-MOSFETs,[31] and *n*-FETs prepared in a similar way also outperform conventional Si *n*-MOSFETs.[273]

Applications of NM arrays for directed cellular growth have been intensively studied,[41−43,276−278] and further electrical studies of action potentials for neuronal networks typically incorporate arrays of microelectrodes.[43,279−281] An alternative optical detection method with much improved signal-to-noise ratios has been described by Koitmäe and co-workers;[276] using a heterostructure of GaAs/InAlGaAs self-rolled as a nanotube with an optically active GaAs QW region.[276] Encapsulated with PDMS and parylene-C to prevent cell toxicity,[40] cerebellar granule neurons were selectively plated to regions patterned with poly-L-lysine (PLL), showing chemical and geometric cues for neurite outgrowth around and inside of the nanotubes (Figure 7f). The growth can then be monitored optically via confocal microscopy, as seen on the right in Figure 7f, where the thinness of the nanotubes allows sufficient transparency to monitor cell dynamics within the tubes. In this way, axons growing on the outside of the tubes (shown in red), axons growing inside of the tube (shown in blue), and empty tubes (shown in black) can be easily discriminated. A very recent paper has shown direct neurophysiology studies being carried out on NM microcellular frameworks that were used to support and reassemble multicellular tissue mimetic organizations of dorsal root ganglia.[196] Schemes for geometrical and chemical cues for directed growth of cellular networks can be extended very broadly to other material sets and other cell types as well, results that show an emerging area of opportunity for the use and integration of NMs with living tissue.[42,244,282−287]

4. CONCLUSION

In this Perspective, we have discussed strategies that embody unique frameworks for next-generation electronic and optoelectronic devices. The use of semiconductor NMs facilitates these unique frameworks in such a way that utilizes the knowledge base from years of processing optimization and builds upon it, expanding device applications to stretchable and flexible electronics, spintronic and valleytronic electronics, transient devices, etc. Applications have taken inspiration from biology, compressively buckling Si NMs into a variety of unique architectures that still retain electrical performance characteristics rivaling that of rigid and planar integrated circuits. Further, NMs have been incorporated into biological studies in which electrical devices are implanted and dissolve over controlled time scales, or into studies that utilize the unique rolled-up architectures of semiconductor NMs to direct growth of cellular and neuronal networks. Atomically thin materials are relatively new as compared to NMs prepared via traditional patterning and etching techniques, but a sufficient amount of progress has been made on synthesis and passivation techniques that improve mobilities and the physical lifetime of the material prior to degradation. The transparency of ML materials is attractive for a variety of applications and moreover, is impressive when the absorptivity of the materials is considered. Transparent photovoltaics and LEDs could be possible with MoS_2, for example. These results foreshadow a future for soft electronics with characteristics and features that are profoundly different from those existing ones and thus offer broad societal implications.

These aspects of semiconductor NMs are quite promising for future electronic and optoelectronic devices, but future work on synthesis of high quality, high-throughput NMs is needed prior to large-scale fabrication for industrial applications. In particular, the synthesis of 2D materials largely focuses on exfoliation techniques to produce the highest quality material; however, when attempting large-scale vapor- or liquid-based synthesis techniques, the device performance suffers. With these improvements, NMs provide opportunities for unique forms of function that exploit the NM figures of merit. These opportunities include flexible, wearable electronics, bioelectronic integration, spintronic and quantum devices, transparent optoelectronics, and nanoelectronics that could not be realized with their bulk counterparts.

AUTHOR INFORMATION

Corresponding Authors

*r-nuzzo@illinois.edu
*jrogers@northwestern.edu

ORCID

Mikayla A. Yoder: 0000-0003-0470-6388

Notes

The authors declare no competing financial interest.

ACKNOWLEDGMENTS

This work was supported by the "Light-Material Interactions in Energy Conversion" Energy Frontier Research Center funded by the U.S. Department of Energy, Office of Science, Office of Basic Energy Sciences under Award Number DE-SC0001293 (subcontract no. 67N-1087758).

REFERENCES

(1) Rogers, J. A.; Lagally, M. G.; Nuzzo, R. G. *Nature* **2011**, *477* (7362), 45−53.
(2) Kim, D. H.; Rogers, J. A. *ACS Nano* **2009**, *3* (3), 498−501.
(3) He, J.; Nuzzo, R. G.; Rogers, J. A. *Proc. IEEE* **2015**, *103* (4), 619−632.
(4) Wang, X.; Chen, Y.; Schmidt, O. G.; Yan, C. *Chem. Soc. Rev.* **2016**, *45* (5), 1308−1330.
(5) Sun, Y.; Rogers, J. A. *Adv. Mater.* **2007**, *19* (15), 1897−1916.
(6) Hwang, S. W.; Tao, H.; Kim, D. H.; Cheng, H. Y.; Song, J. K.; Rill, E.; Brenckle, M. A.; Panilaitis, B.; Won, S. M.; Kim, Y. S.; Song, Y. M.; Yu, K. J.; Ameen, A.; Li, R.; Su, Y. W.; Yang, M. M.; Kaplan, D. L.; Zakin, M. R.; Slepian, M. J.; Huang, Y. G.; Omenetto, F. G.; Rogers, J. A. *Science* **2012**, *337* (6102), 1640−1644.
(7) Hwang, S. W.; Park, G.; Edwards, C.; Corbin, E. A.; Kang, S.; Cheng, H.; Song, J.; Kim, J.; Yu, S.; Ng, J.; Lee, J. E.; Kim, J.; Yee, C.;

DOI: 10.1021/jacs.8b04225
J. Am. Chem. Soc. 2018, 140, 9001−9019

Bhaduri, B.; Su, Y.; Omennetto, F. G.; Huang, Y.; Bashir, R.; Goddard, L.; Popescu, G.; Lee, K. J.; Rogers, J. A. *ACS Nano* **2014**, *8* (6), 5843−5851.
(8) Jang, H.; Lee, W.; Won, S. M.; Ryu, S. Y.; Lee, D.; Koo, J. B.; Ahn, S. D.; Yang, C. W.; Jo, M. H.; Cho, J. H.; Rogers, J. A.; Ahn, J. H. *Nano Lett.* **2013**, *13* (11), 5600−7.
(9) Kim, T.-i.; Kim, M. J.; Jung, Y. H.; Jang, H.; Dagdeviren, C.; Pao, H. A.; Cho, S. J.; Carlson, A.; Yu, K. J.; Ameen, A.; Chung, H.-j.; Jin, S. H.; Ma, Z.; Rogers, J. A. *Chem. Mater.* **2014**, *26* (11), 3502−3507.
(10) Jariwala, D.; Sangwan, V. K.; Lauhon, L. J.; Marks, T. J.; Hersam, M. C. *ACS Nano* **2014**, *8* (2), 1102−1120.
(11) Wang, Q. H.; Kalantar-Zadeh, K.; Kis, A.; Coleman, J. N.; Strano, M. S. *Nat. Nanotechnol.* **2012**, *7* (11), 699−712.
(12) Sanchez-Perez, J. R.; Boztug, C.; Chen, F.; Sudradjat, F. F.; Paskiewicz, D. M.; Jacobson, R. B.; Lagally, M. G.; Paiella, R. *Proc. Natl. Acad. Sci. U. S. A.* **2011**, *108* (47), 18893−8.
(13) Roberts, M. M.; Klein, L. J.; Savage, D. E.; Slinker, K. A.; Friesen, M.; Celler, G.; Eriksson, M. A.; Lagally, M. G. *Nat. Mater.* **2006**, *5* (5), 388−93.
(14) Sookchoo, P.; Sudradjat, F. F.; Kiefer, A. M.; Durmaz, H.; Paiella, R.; Lagally, M. G. *ACS Nano* **2013**, *7* (3), 2326−2334.
(15) Li, X. *Adv. Opt. Photonics* **2011**, *3* (4), 366.
(16) Li, X. *J. Phys. D: Appl. Phys.* **2008**, *41* (19), 193001.
(17) Chhowalla, M.; Shin, H. S.; Eda, G.; Li, L.-J.; Loh, K. P.; Zhang, H. *Nat. Chem.* **2013**, *5* (4), 263−275.
(18) Chen, F.; Ramayya, E. B.; Euaruksakul, C.; Himpsel, F. J.; Celler, G.; Ding, B.; Knezevic, I.; Lagally, M. G. *ACS Nano* **2010**, *4* (4), 2466−2474.
(19) Ling, X.; Wang, H.; Huang, S.; Xia, F.; Dresselhaus, M. S. *Proc. Natl. Acad. Sci. U. S. A.* **2015**, *112* (15), 4523−4530.
(20) Kane, M. G. Organic and Polymeric TFTs for Flexible Displays and Circuits. In *Flexible Electronics: Materials and Applications*; Wong, W. S., Salleo, A., Eds.; Springer Science+Business Media, 2009.
(21) Mak, K. F.; Shan, J. *Nat. Photonics* **2016**, *10* (4), 216−226.
(22) Xia, F.; Wang, H.; Jia, Y. *Nat. Commun.* **2014**, *5*, 4458.
(23) Balendhran, S.; Walia, S.; Nili, H.; Sriram, S.; Bhaskaran, M. *Small* **2015**, *11* (6), 640−652.
(24) Kara, A.; Enriquez, H.; Seitsonen, A. P.; Lew Yan Voon, L. C.; Vizzini, S.; Aufray, B.; Oughaddou, H. *Surf. Sci. Rep.* **2012**, *67* (1), 1−18.
(25) Kim, D. H.; Lu, N. S.; Ma, R.; Kim, Y. S.; Kim, R. H.; Wang, S. D.; Wu, J.; Won, S. M.; Tao, H.; Islam, A.; Yu, K. J.; Kim, T. I.; Chowdhury, R.; Ying, M.; Xu, L. Z.; Li, M.; Chung, H. J.; Keum, H.; McCormick, M.; Liu, P.; Zhang, Y. W.; Omenetto, F. G.; Huang, Y. G.; Coleman, T.; Rogers, J. A. *Science* **2011**, *333* (6044), 838−843.
(26) Kim, J.; Banks, A.; Cheng, H.; Xie, Z.; Xu, S.; Jang, K.-I.; Lee, J. W.; Liu, Z.; Gutruf, P.; Huang, X.; Wei, P.; Liu, F.; Li, K.; Dalal, M.; Ghaffari, R.; Feng, X.; Huang, Y.; Gupta, S.; Paik, U.; Rogers, J. A. *Small* **2015**, *11* (8), 906−912.
(27) Xu, S.; Zhang, Y. H.; Jia, L.; Mathewson, K. E.; Jang, K. I.; Kim, J.; Fu, H. R.; Huang, X.; Chava, P.; Wang, R. H.; Bhole, S.; Wang, L. Z.; Na, Y. J.; Guan, Y.; Flavin, M.; Han, Z. S.; Huang, Y. G.; Rogers, J. A. *Science* **2014**, *344* (6179), 70−74.
(28) Kim, H. S.; Brueckner, E.; Song, J.; Li, Y.; Kim, S.; Lu, C.; Sulkin, J.; Choquette, K.; Huang, Y.; Nuzzo, R. G.; Rogers, J. A. *Proc. Natl. Acad. Sci. U. S. A.* **2011**, *108* (25), 10072−7.
(29) Park, S.-I.; Xiong, Y.; Kim, R.-H.; Elvikis, P.; Meitl, M.; Kim, D.-H.; Wu, J.; Yoon, J.; Yu, C.-J.; Liu, Z.; Huang, Y.; Hwang, K.-c.; Ferreira, P.; Li, X.; Choquette, K.; Rogers, J. A. *Science* **2009**, *325* (5943), 977−981.
(30) Nah, J.; Fang, H.; Wang, C.; Takei, K.; Lee, M. H.; Plis, E.; Krishna, S.; Javey, A. *Nano Lett.* **2012**, *12* (7), 3592−5.
(31) Takei, K.; Madsen, M.; Fang, H.; Kapadia, R.; Chuang, S.; Kim, H. S.; Liu, C. H.; Plis, E.; Nah, J.; Krishna, S.; Chueh, Y. L.; Guo, J.; Javey, A. *Nano Lett.* **2012**, *12* (4), 2060−6.
(32) Knapp, T. J.; Mohr, R. T.; Li, Y. S.; Thorgrimsson, B.; Foote, R. H.; Wu, X.; Ward, D. R.; Savage, D. E.; Lagally, M. G.; Friesen, M.; Coppersmith, S. N.; Eriksson, M. A. *Nanotechnology* **2016**, *27*, 154002.
(33) Whitney, W. S.; Sherrott, M. C.; Jariwala, D.; Lin, W.-H.; Bechtel, H. A.; Rossman, G. R.; Atwater, H. A. *Nano Lett.* **2017**, *17* (1), 78−84.
(34) Radosavljevic, M.; Ashley, T.; Andreev, A.; Coomber, S. D.; Dewey, G.; Emeny, M. T.; Fearn, M.; Hayes, D. G.; Hilton, K. P.; Hudait, M. K.; Jefferies, R.; Martin, T.; Pillarisetty, R.; Rachmady, W.; Rakshit, T.; Smith, S. J.; Uren, M. J.; Wallis, D. J.; Wilding, P. J.; Chau, R. High-performance 40nm gate length InSb p-channel compressively strained quantum well field effect transistors for low-power (VCC = 0.5V) logic applications. *2008 IEEE International Electron Devices Meeting*, San Francisco, CA, December 15−17, 2008; pp 1−4.
(35) Sigg, H. Intersubband Transitions in Si/SiGe Heterojunctions, Quantum Dots, and Quantum Wells. In *Intersubband Transitions in Quantum Structures*; Paiella, R., Ed.; McGraw-Hill, 2006; pp 347−388.
(36) Favron, A.; Gaufres, E.; Fossard, F.; Phaneuf-L'heureux, A.-L.; Tang, N. Y. W.; Levesque, P. L.; Loiseau, A.; Leonelli, R.; Francoeur, S.; Martel, R. *Nat. Mater.* **2015**, *14* (8), 826−832.
(37) Li, L.; Yang, F.; Ye, G. J.; Zhang, Z.; Zhu, Z.; Lou, W.; Zhou, X.; Li, L.; Watanabe, K.; Taniguchi, T.; Chang, K.; Wang, Y.; Chen, X. H.; Zhang, Y. *Nat. Nanotechnol.* **2016**, *11* (7), 593−597.
(38) Liu, C.-C.; Feng, W.; Yao, Y. *Phys. Rev. Lett.* **2011**, *107* (7), 076802.
(39) Ezawa, M. *Phys. Rev. Lett.* **2012**, *109* (5), 055502.
(40) Bausch, C. S.; Koitmäe, A.; Stava, E.; Price, A.; Resto, P. J.; Huang, Y.; Sonnenberg, D.; Stark, Y.; Heyn, C.; Williams, J. C.; Dent, E. W.; Blick, R. H. *Appl. Phys. Lett.* **2013**, *103* (17), 173705.
(41) Yu, M.; Huang, Y.; Ballweg, J.; Shin, H.; Huang, M.; Savage, D. E.; Lagally, M. G.; Dent, E. W.; Blick, R. H.; Williams, J. C. *ACS Nano* **2011**, *5* (4), 2447−57.
(42) Froeter, P.; Huang, Y.; Cangellaris, O. V.; Huang, W.; Dent, E. W.; Gillette, M. U.; Williams, J. C.; Li, X. *ACS Nano* **2014**, *8* (11), 11108−11117.
(43) Cavallo, F.; Huang, Y.; Dent, E. W.; Williams, J. C.; Lagally, M. G. *ACS Nano* **2014**, *8* (12), 12219−12227.
(44) Tan, C.; Cao, X.; Wu, X.-J.; He, Q.; Yang, J.; Zhang, X.; Chen, J.; Zhao, W.; Han, S.; Nam, G.-H.; Sindoro, M.; Zhang, H. *Chem. Rev.* **2017**, *117* (9), 6225−6331.
(45) Chhowalla, M.; Jena, D.; Zhang, H. *Nat. Rev. Mater.* **2016**, *1*, 16052.
(46) Song, X.; Hu, J.; Zeng, H. *J. Mater. Chem. C* **2013**, *1* (17), 2952−2969.
(47) Fiori, G.; Bonaccorso, F.; Iannaccone, G.; Palacios, T.; Neumaier, D.; Seabaugh, A.; Banerjee, S. K.; Colombo, L. *Nat. Nanotechnol.* **2014**, *9* (10), 768−779.
(48) Yan, Z.; Han, M.; Yang, Y.; Nan, K.; Luan, H.; Luo, Y.; Zhang, Y.; Huang, Y.; Rogers, J. A. *Extreme Mechanics Letters* **2017**, *11*, 96−104.
(49) Rogers, J. A.; Someya, T.; Huang, Y. *Science* **2010**, *327* (5973), 1603−1607.
(50) Zhang, Y.; Zhang, F.; Yan, Z.; Ma, Q.; Li, X.; Huang, Y.; Rogers, J. A. *Nat. Rev. Mater.* **2017**, *2*, 17019.
(51) Novoselov, K. S.; Geim, A. K.; Morozov, S. V.; Jiang, D.; Zhang, Y.; Dubonos, S. V.; Grigorieva, I. V.; Firsov, A. A. *Science* **2004**, *306* (5696), 666−669.
(52) Hernandez, Y.; Nicolosi, V.; Lotya, M.; Blighe, F. M.; Sun, Z.; De, S.; McGovern, I. T.; Holland, B.; Byrne, M.; Gun'Ko, Y. K.; Boland, J. J.; Niraj, P.; Duesberg, G.; Krishnamurthy, S.; Goodhue, R.; Hutchison, J.; Scardaci, V.; Ferrari, A. C.; Coleman, J. N. *Nat. Nanotechnol.* **2008**, *3* (9), 563−568.
(53) Chandrashekar, B. N.; Deng, B.; Smitha, A. S.; Chen, Y.; Tan, C.; Zhang, H.; Peng, H.; Liu, Z. *Adv. Mater.* **2015**, *27* (35), 5210−5216.
(54) Alrefae, M. A.; Kumar, A.; Pandita, P.; Candadai, A.; Bilionis, I.; Fisher, T. S. *AIP Adv.* **2017**, *7* (11), 115102.
(55) Kobayashi, T.; Bando, M.; Kimura, N.; Shimizu, K.; Kadono, K.; Umezu, N.; Miyahara, K.; Hayazaki, S.; Nagai, S.; Mizuguchi, Y.; Murakami, Y.; Hobara, D. *Appl. Phys. Lett.* **2013**, *102* (2), 023112.
(56) Vlassiouk, I.; Fulvio, P.; Meyer, H.; Lavrik, N.; Dai, S.; Datskos, P.; Smirnov, S. *Carbon* **2013**, *54*, 58−67.

DOI: 10.1021/jacs.8b04225
J. Am. Chem. Soc. 2018, 140, 9001−9019

(57) Yamada, T.; Ishihara, M.; Kim, J.; Hasegawa, M.; Iijima, S. *Carbon* **2012**, *50* (7), 2615−2619.
(58) Hesjedal, T. *Appl. Phys. Lett.* **2011**, *98* (13), 133106.
(59) Polsen, E. S.; McNerny, D. Q.; Viswanath, B.; Pattinson, S. W.; John Hart, A. *Sci. Rep.* **2015**, *5*, 10257.
(60) Ko, H. C.; Baca, A. J.; Rogers, J. A. *Nano Lett.* **2006**, *6* (10), 2318.
(61) Fang, H.; Zhao, J.; Yu, K. J.; Song, E.; Farimani, A. B.; Chiang, C.-H.; Jin, X.; Xue, Y.; Xu, D.; Du, W.; Seo, K. J.; Zhong, Y.; Yang, Z.; Won, S. M.; Fang, G.; Choi, S. W.; Chaudhuri, S.; Huang, Y.; Alam, M. A.; Viventi, J.; Aluru, N. R.; Rogers, J. A. *Proc. Natl. Acad. Sci. U. S. A.* **2016**, *113* (42), 11682−11687.
(62) Yablonovitch, E.; Gmitter, T.; Harbison, J. P.; Bhat, R. *Appl. Phys. Lett.* **1987**, *51* (26), 2222.
(63) Yang, H.; Zhao, D.; Chuwongin, S.; Seo, J.-H.; Yang, W.; Shuai, Y.; Berggren, J.; Hammar, M.; Ma, Z.; Zhou, W. *Nat. Photonics* **2012**, *6* (9), 615−620.
(64) Khang, D.-Y.; Jiang, H.; Huang, Y.; Rogers, J. A. *Science* **2006**, *311* (5758), 208−212.
(65) Yan, Z.; Zhang, F.; Wang, J.; Liu, F.; Guo, X.; Nan, K.; Lin, Q.; Gao, M.; Xiao, D.; Shi, Y.; Qiu, Y.; Luan, H.; Kim, J. H.; Wang, Y.; Luo, H.; Han, M.; Huang, Y.; Zhang, Y.; Rogers, J. A. *Adv. Funct. Mater.* **2016**, *26* (16), 2629−2639.
(66) Zhang, S.; Yang, J.; Xu, R.; Wang, F.; Li, W.; Ghufran, M.; Zhang, Y.-W.; Yu, Z.; Zhang, G.; Qin, Q.; Lu, Y. *ACS Nano* **2014**, *8* (9), 9590−9596.
(67) Deng, Y.; Luo, Z.; Conrad, N. J.; Liu, H.; Gong, Y.; Najmaei, S.; Ajayan, P. M.; Lou, J.; Xu, X.; Ye, P. D. *ACS Nano* **2014**, *8* (8), 8292−8299.
(68) Dai, J.; Zeng, X. C. *J. Phys. Chem. Lett.* **2014**, *5* (7), 1289−1293.
(69) Yuan, H.; Liu, X.; Afshinmanesh, F.; Li, W.; Xu, G.; Sun, J.; Lian, B.; Curto, A. G.; Ye, G.; Hikita, Y.; Shen, Z.; Zhang, S.-C.; Chen, X.; Brongersma, M.; Hwang, H. Y.; Cui, Y. *Nat. Nanotechnol.* **2015**, *10* (8), 707−713.
(70) Yin, Z.; Li, H.; Li, H.; Jiang, L.; Shi, Y.; Sun, Y.; Lu, G.; Zhang, Q.; Chen, X.; Zhang, H. *ACS Nano* **2012**, *6* (1), 74−80.
(71) Ross, J. S.; Klement, P.; Jones, A. M.; Ghimire, N. J.; Yan, J.; Mandrus, D. G.; Taniguchi, T.; Watanabe, K.; Kitamura, K.; Yao, W.; Cobden, D. H.; Xu, X. *Nat. Nanotechnol.* **2014**, *9* (4), 268−272.
(72) Sundaram, R. S.; Engel, M.; Lombardo, A.; Krupke, R.; Ferrari, A. C.; Avouris, P.; Steiner, M. *Nano Lett.* **2013**, *13* (4), 1416−1421.
(73) Fontana, M.; Deppe, T.; Boyd, A. K.; Rinzan, M.; Liu, A. Y.; Paranjape, M.; Barbara, P. *Sci. Rep.* **2013**, *3*, 1634.
(74) Wi, S.; Kim, H.; Chen, M.; Nam, H.; Guo, L. J.; Meyhofer, E.; Liang, X. *ACS Nano* **2014**, *8* (5), 5270−5281.
(75) Choi, W.; Cho, M. Y.; Konar, A.; Lee, J. H.; Cha, G.-B.; Hong, S. C.; Kim, S.; Kim, J.; Jena, D.; Joo, J.; Kim, S. *Adv. Mater.* **2012**, *24* (43), 5832−5836.
(76) Yu, W. J.; Liu, Y.; Zhou, H.; Yin, A.; Li, Z.; Huang, Y.; Duan, X. *Nat. Nanotechnol.* **2013**, *8* (12), 952−958.
(77) Withers, F.; Del Pozo-Zamudio, O.; Mishchenko, A.; Rooney, A. P.; Gholinia, A.; Watanabe, K.; Taniguchi, T.; Haigh, S. J.; Geim, A. K.; Tartakovskii, A. I.; Novoselov, K. S. *Nat. Mater.* **2015**, *14* (3), 301−306.
(78) Jo, S.; Ubrig, N.; Berger, H.; Kuzmenko, A. B.; Morpurgo, A. F. *Nano Lett.* **2014**, *14* (4), 2019−2025.
(79) Lee, H. S.; Min, S.-W.; Chang, Y.-G.; Park, M. K.; Nam, T.; Kim, H.; Kim, J. H.; Ryu, S.; Im, S. *Nano Lett.* **2012**, *12* (7), 3695−3700.
(80) Jariwala, D.; Davoyan, A. R.; Tagliabue, G.; Sherrott, M. C.; Wong, J.; Atwater, H. A. *Nano Lett.* **2016**, *16* (9), 5482−5487.
(81) Baugher, B. W. H.; Churchill, H. O. H.; Yang, Y.; Jarillo-Herrero, P. *Nat. Nanotechnol.* **2014**, *9* (4), 262−267.
(82) Pospischil, A.; Furchi, M. M.; Mueller, T. *Nat. Nanotechnol.* **2014**, *9* (4), 257−261.
(83) Radisavljevic, B.; Radenovic, A.; Brivio, J.; Giacometti, V.; Kis, A. *Nat. Nanotechnol.* **2011**, *6* (3), 147−150.
(84) Das, S.; Chen, H.-Y.; Penumatcha, A. V.; Appenzeller, J. *Nano Lett.* **2013**, *13* (1), 100−105.
(85) Pradhan, N. R.; Rhodes, D.; Xin, Y.; Memaran, S.; Bhaskaran, L.; Siddiq, M.; Hill, S.; Ajayan, P. M.; Balicas, L. *ACS Nano* **2014**, *8* (8), 7923−7929.
(86) Fang, H.; Tosun, M.; Seol, G.; Chang, T. C.; Takei, K.; Guo, J.; Javey, A. *Nano Lett.* **2013**, *13* (5), 1991−1995.
(87) Allain, A.; Kis, A. *ACS Nano* **2014**, *8* (7), 7180−7185.
(88) Pradhan, N. R.; Rhodes, D.; Memaran, S.; Poumirol, J. M.; Smirnov, D.; Talapatra, S.; Feng, S.; Perea-Lopez, N.; Elias, A. L.; Terrones, M.; Ajayan, P. M.; Balicas, L. *Sci. Rep.* **2015**, *5*, 8979.
(89) Fang, H.; Chuang, S.; Chang, T. C.; Takei, K.; Takahashi, T.; Javey, A. *Nano Lett.* **2012**, *12* (7), 3788−3792.
(90) Radisavljevic, B.; Kis, A. *Nat. Mater.* **2013**, *12* (9), 815−820.
(91) Cui, X.; Lee, G.-H.; Kim, Y. D.; Arefe, G.; Huang, P. Y.; Lee, C.-H.; Chenet, D. A.; Zhang, X.; Wang, L.; Ye, F.; Pizzocchero, F.; Jessen, B. S.; Watanabe, K.; Taniguchi, T.; Muller, D. A.; Low, T.; Kim, P.; Hone, J. *Nat. Nanotechnol.* **2015**, *10* (6), 534−540.
(92) Avsar, A.; Vera-Marun, I. J.; Tan, J. Y.; Watanabe, K.; Taniguchi, T.; Castro Neto, A. H.; Özyilmaz, B. *ACS Nano* **2015**, *9* (4), 4138−4145.
(93) Li, L.; Yu, Y.; Ye, G. J.; Ge, Q.; Ou, X.; Wu, H.; Feng, D.; Chen, X. H.; Zhang, Y. *Nat. Nanotechnol.* **2014**, *9* (5), 372−377.
(94) Zhu, W.; Yogeesh, M. N.; Yang, S.; Aldave, S. H.; Kim, J.-S.; Sonde, S.; Tao, L.; Lu, N.; Akinwande, D. *Nano Lett.* **2015**, *15* (3), 1883−1890.
(95) Wood, J. D.; Wells, S. A.; Jariwala, D.; Chen, K.-S.; Cho, E.; Sangwan, V. K.; Liu, X.; Lauhon, L. J.; Marks, T. J.; Hersam, M. C. *Nano Lett.* **2014**, *14* (12), 6964−6970.
(96) Liu, H.; Neal, A. T.; Si, M.; Du, Y.; Ye, P. D. *IEEE Electron Device Lett.* **2014**, *35* (7), 795−797.
(97) Koenig, S. P.; Doganov, R. A.; Schmidt, H.; Castro Neto, A. H.; Özyilmaz, B. *Appl. Phys. Lett.* **2014**, *104* (10), 103106.
(98) Wang, X.; Jones, A. M.; Seyler, K. L.; Tran, V.; Jia, Y.; Zhao, H.; Wang, H.; Yang, L.; Xu, X.; Xia, F. *Nat. Nanotechnol.* **2015**, *10* (6), 517−521.
(99) Doganov, R. A.; O'Farrell, E. C. T.; Koenig, S. P.; Yeo, Y.; Ziletti, A.; Carvalho, A.; Campbell, D. K.; Coker, D. F.; Watanabe, K.; Taniguchi, T.; Neto, A. H. C.; Özyilmaz, B. *Nat. Commun.* **2015**, *6*, 6647.
(100) Chen, X.; Wu, Y.; Wu, Z.; Han, Y.; Xu, S.; Wang, L.; Ye, W.; Han, T.; He, Y.; Cai, Y.; Wang, N. *Nat. Commun.* **2015**, *6*, 7315.
(101) Coleman, J. N.; Lotya, M.; O'Neill, A.; Bergin, S. D.; King, P. J.; Khan, U.; Young, K.; Gaucher, A.; De, S.; Smith, R. J.; Shvets, I. V.; Arora, S. K.; Stanton, G.; Kim, H.-Y.; Lee, K.; Kim, G. T.; Duesberg, G. S.; Hallam, T.; Boland, J. J.; Wang, J. J.; Donegan, J. F.; Grunlan, J. C.; Moriarty, G.; Shmeliov, A.; Nicholls, R. J.; Perkins, J. M.; Grieveson, E. M.; Theuwissen, K.; McComb, D. W.; Nellist, P. D.; Nicolosi, V. *Science* **2011**, *331* (6017), 568−571.
(102) Bergin, S. D.; Sun, Z.; Rickard, D.; Streich, P. V.; Hamilton, J. P.; Coleman, J. N. *ACS Nano* **2009**, *3* (8), 2340−2350.
(103) Hernandez, Y.; Lotya, M.; Rickard, D.; Bergin, S. D.; Coleman, J. N. *Langmuir* **2010**, *26* (5), 3208−3213.
(104) Kim, C.; Nguyen, T. P.; Le, Q. V.; Jeon, J.-M.; Jang, H. W.; Kim, S. Y. *Adv. Funct. Mater.* **2015**, *25* (28), 4512−4519.
(105) Lee, K.; Kim, H.-Y.; Lotya, M.; Coleman, J. N.; Kim, G.-T.; Duesberg, G. S. *Adv. Mater.* **2011**, *23* (36), 4178−4182.
(106) Nicolosi, V.; Chhowalla, M.; Kanatzidis, M. G.; Strano, M. S.; Coleman, J. N. *Science* **2013**, *340* (6139), 1226419.
(107) Guo, Z.; Zhang, H.; Lu, S.; Wang, Z.; Tang, S.; Shao, J.; Sun, Z.; Xie, H.; Wang, H.; Yu, X.-F.; Chu, P. K. *Adv. Funct. Mater.* **2015**, *25* (45), 6996−7002.
(108) Hanlon, D.; Backes, C.; Doherty, E.; Cucinotta, C. S.; Berner, N. C.; Boland, C.; Lee, K.; Harvey, A.; Lynch, P.; Gholamvand, Z.; Zhang, S.; Wang, K.; Moynihan, G.; Pokle, A.; Ramasse, Q. M.; McEvoy, N.; Blau, W. J.; Wang, J.; Abellan, G.; Hauke, F.; Hirsch, A.; Sanvito, S.; O'Regan, D. D.; Duesberg, G. S.; Nicolosi, V.; Coleman, J. N. *Nat. Commun.* **2015**, *6*, 8563.
(109) Kang, J.; Wood, J. D.; Wells, S. A.; Lee, J.-H.; Liu, X.; Chen, K.-S.; Hersam, M. C. *ACS Nano* **2015**, *9* (4), 3596−3604.

DOI: 10.1021/jacs.8b04225
J. Am. Chem. Soc. 2018, 140, 9001−9019

(110) Yasaei, P.; Kumar, B.; Foroozan, T.; Wang, C.; Asadi, M.; Tuschel, D.; Indacochea, J. E.; Klie, R. F.; Salehi-Khojin, A. *Adv. Mater.* **2015**, *27* (11), 1887−1892.
(111) Brent, J. R.; Savjani, N.; Lewis, E. A.; Haigh, S. J.; Lewis, D. J.; O'Brien, P. *Chem. Commun.* **2014**, *50* (87), 13338−13341.
(112) Smith, R. J.; King, P. J.; Lotya, M.; Wirtz, C.; Khan, U.; De, S.; O'Neill, A.; Duesberg, G. S.; Grunlan, J. C.; Moriarty, G.; Chen, J.; Wang, J.; Minett, A. I.; Nicolosi, V.; Coleman, J. N. *Adv. Mater.* **2011**, *23* (34), 3944−3948.
(113) Julien, C. M. *Mater. Sci. Eng., R* **2003**, *40* (2), 47−102.
(114) Chrissafis, K.; Zamani, M.; Kambas, K.; Stoemenos, J.; Economou, N. A.; Samaras, I.; Julien, C. *Mater. Sci. Eng., B* **1989**, *3* (1), 145−151.
(115) Fan, X.; Xu, P.; Zhou, D.; Sun, Y.; Li, Y. C.; Nguyen, M. A. T.; Terrones, M.; Mallouk, T. E. *Nano Lett.* **2015**, *15* (9), 5956−5960.
(116) Zeng, Z.; Yin, Z.; Huang, X.; Li, H.; He, Q.; Lu, G.; Boey, F.; Zhang, H. *Angew. Chem., Int. Ed.* **2011**, *50* (47), 11093−11097.
(117) Joensen, P.; Frindt, R. F.; Morrison, S. R. *Mater. Res. Bull.* **1986**, *21* (4), 457−461.
(118) Ramakrishna Matte, H. S. S.; Gomathi, A.; Manna, A. K.; Late, D. J.; Datta, R.; Pati, S. K.; Rao, C. N. R. *Angew. Chem.* **2010**, *122* (24), 4153−4156.
(119) Fan, X.; Xu, P.; Li, Y. C.; Zhou, D.; Sun, Y.; Nguyen, M. A. T.; Terrones, M.; Mallouk, T. E. *J. Am. Chem. Soc.* **2016**, *138* (15), 5143−5149.
(120) Gholamvand, Z.; McAteer, D.; Backes, C.; McEvoy, N.; Harvey, A.; Berner, N. C.; Hanlon, D.; Bradley, C.; Godwin, I.; Rovetta, A.; Lyons, M. E. G.; Duesberg, G. S.; Coleman, J. N. *Nanoscale* **2016**, *8* (10), 5737−5749.
(121) Lukowski, M. A.; Daniel, A. S.; Meng, F.; Forticaux, A.; Li, L.; Jin, S. *J. Am. Chem. Soc.* **2013**, *135* (28), 10274−10277.
(122) Eda, G.; Yamaguchi, H.; Voiry, D.; Fujita, T.; Chen, M.; Chhowalla, M. *Nano Lett.* **2011**, *11* (12), 5111−5116.
(123) Zeng, Z.; Sun, T.; Zhu, J.; Huang, X.; Yin, Z.; Lu, G.; Fan, Z.; Yan, Q.; Hng, H. H.; Zhang, H. *Angew. Chem., Int. Ed.* **2012**, *51* (36), 9052−9056.
(124) Dines, M. B. *Mater. Res. Bull.* **1975**, *10* (4), 287−291.
(125) Lee, Y. H.; Zhang, X. Q.; Zhang, W.; Chang, M. T.; Lin, C. T.; Chang, K. D.; Yu, Y. C.; Wang, J. T.; Chang, C. S.; Li, L. J.; Lin, T. W. *Adv. Mater.* **2012**, *24* (17), 2320−5.
(126) Najmaei, S.; Liu, Z.; Zhou, W.; Zou, X.; Shi, G.; Lei, S.; Yakobson, B. I.; Idrobo, J.-C.; Ajayan, P. M.; Lou, J. *Nat. Mater.* **2013**, *12* (8), 754−759.
(127) Zhan, Y.; Liu, Z.; Najmaei, S.; Ajayan, P. M.; Lou, J. *Small* **2012**, *8* (7), 966−971.
(128) Liu, K.-K.; Zhang, W.; Lee, Y.-H.; Lin, Y.-C.; Chang, M.-T.; Su, C.-Y.; Chang, C.-S.; Li, H.; Shi, Y.; Zhang, H.; Lai, C.-S.; Li, L.-J. *Nano Lett.* **2012**, *12* (3), 1538−1544.
(129) Shi, Y.; Zhou, W.; Lu, A.-Y.; Fang, W.; Lee, Y.-H.; Hsu, A. L.; Kim, S. M.; Kim, K. K.; Yang, H. Y.; Li, L.-J.; Idrobo, J.-C.; Kong, J. *Nano Lett.* **2012**, *12* (6), 2784−2791.
(130) Lin, Y.-C.; Zhang, W.; Huang, J.-K.; Liu, K.-K.; Lee, Y.-H.; Liang, C.-T.; Chu, C.-W.; Li, L.-J. *Nanoscale* **2012**, *4* (20), 6637−6641.
(131) Schmidt, H.; Wang, S.; Chu, L.; Toh, M.; Kumar, R.; Zhao, W.; Castro Neto, A. H.; Martin, J.; Adam, S.; Özyilmaz, B.; Eda, G. *Nano Lett.* **2014**, *14* (4), 1909−1913.
(132) Wang, X.; Feng, H.; Wu, Y.; Jiao, L. *J. Am. Chem. Soc.* **2013**, *135* (14), 5304−5307.
(133) van der Zande, A. M.; Huang, P. Y.; Chenet, D. A.; Berkelbach, T. C.; You, Y.; Lee, G.-H.; Heinz, T. F.; Reichman, D. R.; Muller, D. A.; Hone, J. C. *Nat. Mater.* **2013**, *12* (6), 554−561.
(134) Wang, S.; Rong, Y.; Fan, Y.; Pacios, M.; Bhaskaran, H.; He, K.; Warner, J. H. *Chem. Mater.* **2014**, *26* (22), 6371−6379.
(135) Ling, X.; Lee, Y.-H.; Lin, Y.; Fang, W.; Yu, L.; Dresselhaus, M. S.; Kong, J. *Nano Lett.* **2014**, *14* (2), 464−472.
(136) Li, L.; Guo, Y.; Sun, Y.; Yang, L.; Qin, L.; Guan, S.; Wang, J.; Qiu, X.; Li, H.; Shang, Y.; Fang, Y. *Adv. Mater.* **2018**, *30* (12), 1706215.
(137) Shim, G. W.; Yoo, K.; Seo, S.-B.; Shin, J.; Jung, D. Y.; Kang, I.-S.; Ahn, C. W.; Cho, B. J.; Choi, S.-Y. *ACS Nano* **2014**, *8* (7), 6655−6662.
(138) Zhang, Y.; Zhang, Y.; Ji, Q.; Ju, J.; Yuan, H.; Shi, J.; Gao, T.; Ma, D.; Liu, M.; Chen, Y.; Song, X.; Hwang, H. Y.; Cui, Y.; Liu, Z. *ACS Nano* **2013**, *7* (10), 8963−8971.
(139) Wang, X.; Gong, Y.; Shi, G.; Chow, W. L.; Keyshar, K.; Ye, G.; Vajtai, R.; Lou, J.; Liu, Z.; Ringe, E.; Tay, B. K.; Ajayan, P. M. *ACS Nano* **2014**, *8* (5), 5125−5131.
(140) Huang, J.-K.; Pu, J.; Hsu, C.-L.; Chiu, M.-H.; Juang, Z.-Y.; Chang, Y.-H.; Chang, W.-H.; Iwasa, Y.; Takenobu, T.; Li, L.-J. *ACS Nano* **2014**, *8* (1), 923−930.
(141) Song, J.-G.; Park, J.; Lee, W.; Choi, T.; Jung, H.; Lee, C. W.; Hwang, S.-H.; Myoung, J. M.; Jung, J.-H.; Kim, S.-H.; Lansalot-Matras, C.; Kim, H. *ACS Nano* **2013**, *7* (12), 11333−11340.
(142) Elías, A. L.; Perea-López, N.; Castro-Beltrán, A.; Berkdemir, A.; Lv, R.; Feng, S.; Long, A. D.; Hayashi, T.; Kim, Y. A.; Endo, M.; Gutiérrez, H. R.; Pradhan, N. R.; Balicas, L.; Mallouk, T. E.; López-Urías, F.; Terrones, H.; Terrones, M. *ACS Nano* **2013**, *7* (6), 5235−5242.
(143) Gutiérrez, H. R.; Perea-López, N.; Elías, A. L.; Berkdemir, A.; Wang, B.; Lv, R.; López-Urías, F.; Crespi, V. H.; Terrones, H.; Terrones, M. *Nano Lett.* **2013**, *13* (8), 3447−3454.
(144) Shaw, J. C.; Zhou, H.; Chen, Y.; Weiss, N. O.; Liu, Y.; Huang, Y.; Duan, X. *Nano Res.* **2014**, *7* (4), 511−517.
(145) Xie, S.; Tu, L.; Han, Y.; Huang, L.; Kang, K.; Lao, K. U.; Poddar, P.; Park, C.; Muller, D. A.; DiStasio, R. A.; Park, J. *Science* **2018**, *359* (6380), 1131−1136.
(146) Kang, K.; Lee, K.-H.; Han, Y.; Gao, H.; Xie, S.; Muller, D. A.; Park, J. *Nature* **2017**, *550*, 229.
(147) Sahoo, P. K.; Memaran, S.; Xin, Y.; Balicas, L.; Gutiérrez, H. R. *Nature* **2018**, *553*, 63.
(148) Zhang, Z.; Chen, P.; Duan, X.; Zang, K.; Luo, J.; Duan, X. *Science* **2017**, *357*, 788−792.
(149) Wang, C.; He, Q.; Halim, U.; Liu, Y.; Zhu, E.; Lin, Z.; Xiao, H.; Duan, X.; Feng, Z.; Cheng, R.; Weiss, N. O.; Ye, G.; Huang, Y.-C.; Wu, H.; Cheng, H.-C.; Shakir, I.; Liao, L.; Chen, X.; Goddard, W. A., III; Huang, Y.; Duan, X. *Nature* **2018**, *555*, 231.
(150) Naylor, C. H.; Parkin, W. M.; Gao, Z.; Berry, J.; Zhou, S.; Zhang, Q.; McClimon, J. B.; Tan, L. Z.; Kehayias, C. E.; Zhao, M.-Q.; Gona, R. S.; Carpick, R. W.; Rappe, A. M.; Srolovitz, D. J.; Drndic, M.; Johnson, A. T. C. *ACS Nano* **2017**, *11* (9), 8619−8627.
(151) Chen, F.; Wang, L.; Ji, X.; Zhang, Q. *ACS Appl. Mater. Interfaces* **2017**, *9* (36), 30821−30831.
(152) Smith, J. B.; Hagaman, D.; Ji, H.-F. *Nanotechnology* **2016**, *27* (21), 215602.
(153) Li, X.; Deng, B.; Wang, X.; Chen, S.; Vaisman, M.; Karato, S.-i.; Pan, G.; Lee, M. L.; Cha, J.; Wang, H.; Xia, F. *2D Mater.* **2015**, *2* (3), 031002.
(154) Yang, Z.; Hao, J.; Yuan, S.; Lin, S.; Yau, H. M.; Dai, J.; Lau, S. P. *Adv. Mater.* **2015**, *27* (25), 3748−3754.
(155) Song, L.; Ci, L.; Lu, H.; Sorokin, P. B.; Jin, C.; Ni, J.; Kvashnin, A. G.; Kvashnin, D. G.; Lou, J.; Yakobson, B. I.; Ajayan, P. M. *Nano Lett.* **2010**, *10* (8), 3209−3215.
(156) Kim, K. K.; Hsu, A.; Jia, X.; Kim, S. M.; Shi, Y.; Hofmann, M.; Nezich, D.; Rodriguez-Nieva, J. F.; Dresselhaus, M.; Palacios, T.; Kong, J. *Nano Lett.* **2012**, *12* (1), 161−166.
(157) Al Balushi, Z. Y.; Wang, K.; Ghosh, R. K.; Vila, R. A.; Eichfeld, S. M.; Caldwell, J. D.; Qin, X.; Lin, Y.-C.; DeSario, P. A.; Stone, G.; Subramanian, S.; Paul, D. F.; Wallace, R. M.; Datta, S.; Redwing, J. M.; Robinson, J. A. *Nat. Mater.* **2016**, *15* (11), 1166−1171.
(158) Novoselov, K. S.; Jiang, D.; Schedin, F.; Booth, T. J.; Khotkevich, V. V.; Morozov, S. V.; Geim, A. K. *Proc. Natl. Acad. Sci. U. S. A.* **2005**, *102* (30), 10451−10453.
(159) Le Lay, G. *Nat. Nanotechnol.* **2015**, *10* (3), 202−203.
(160) Tao, L.; Cinquanta, E.; Chiappe, D.; Grazianetti, C.; Fanciulli, M.; Dubey, M.; Molle, A.; Akinwande, D. *Nat. Nanotechnol.* **2015**, *10* (3), 227−231.

DOI: 10.1021/jacs.8b04225
J. Am. Chem. Soc. 2018, 140, 9001−9019

(161) Drummond, N. D.; Zólyomi, V.; Fal'ko, V. I. *Phys. Rev. B: Condens. Matter Mater. Phys.* **2012**, *85* (7), 075423.
(162) Feng, B.; Ding, Z.; Meng, S.; Yao, Y.; He, X.; Cheng, P.; Chen, L.; Wu, K. *Nano Lett.* **2012**, *12* (7), 3507−3511.
(163) Arafune, R.; Lin, C.-L.; Kawahara, K.; Tsukahara, N.; Minamitani, E.; Kim, Y.; Takagi, N.; Kawai, M. *Surf. Sci.* **2013**, *608*, 297−300.
(164) Kara, A.; Vizzini, S.; Leandri, C.; Ealet, B.; Oughaddou, H.; Aufray, B.; Le Lay, G. *J. Phys.: Condens. Matter* **2010**, *22* (4), 045004.
(165) Aufray, B.; Kara, A.; Vizzini, S.; Oughaddou, H.; Léandri, C.; Ealet, B.; Le Lay, G. *Appl. Phys. Lett.* **2010**, *96* (18), 183102.
(166) Leandri, C.; Lay, G. L.; Aufray, B.; Girardeaux, C.; Avila, J.; Dávila, M. E.; Asensio, M. C.; Ottaviani, C.; Cricenti, A. *Surf. Sci.* **2005**, *574* (1), L9−L15.
(167) Valbuena, M. A.; Avila, J.; Dávila, M. E.; Leandri, C.; Aufray, B.; Le Lay, G.; Asensio, M. C. *Appl. Surf. Sci.* **2007**, *254* (1), 50−54.
(168) Lalmi, B.; Oughaddou, H.; Enriquez, H.; Kara, A.; Vizzini, S.; Ealet, B.; Aufray, B. *Appl. Phys. Lett.* **2010**, *97* (22), 223109.
(169) Takagi, N.; Lin, C.-L.; Kawahara, K.; Minamitani, E.; Tsukahara, N.; Kawai, M.; Arafune, R. *Prog. Surf. Sci.* **2015**, *90* (1), 1−20.
(170) Meng, L.; Wang, Y.; Zhang, L.; Du, S.; Wu, R.; Li, L.; Zhang, Y.; Li, G.; Zhou, H.; Hofer, W. A.; Gao, H.-J. *Nano Lett.* **2013**, *13* (2), 685−690.
(171) Fleurence, A.; Friedlein, R.; Ozaki, T.; Kawai, H.; Wang, Y.; Yamada-Takamura, Y. *Phys. Rev. Lett.* **2012**, *108* (24), 245501.
(172) Hwang, S.-W.; Song, J.-K.; Huang, X.; Cheng, H.; Kang, S.-K.; Kim, B. H.; Kim, J.-H.; Yu, S.; Huang, Y.; Rogers, J. A. *Adv. Mater.* **2014**, *26* (23), 3905−3911.
(173) Mack, S.; Meitl, M. A.; Baca, A. J.; Zhu, Z.-T.; Rogers, J. A. *Appl. Phys. Lett.* **2006**, *88* (21), 213101.
(174) Yoder, M. A.; Yao, Y.; He, J.; Nuzzo, R. G. *Adv. Mater. Technol.* **2017**, *2*, 1700169.
(175) Yao, Y.; Brueckner, E.; Li, L.; Nuzzo, R. *Energy Environ. Sci.* **2013**, *6* (10), 3071.
(176) Franssila, S. *Introduction to Microfabrication*, Second ed.; John Wiley & Sons, Ltd., 2010.
(177) Wind, R. A.; Hines, M. A. *Surf. Sci.* **2000**, *460* (1−3), 21−38.
(178) Keshra, S. *Etching of Crystals*; Elsevier, 1987; Vol. *15*.
(179) Flidr, J.; Huang, Y.-C.; Newton, T. A.; Hines, M. A. *J. Chem. Phys.* **1998**, *108* (13), 5542−5553.
(180) Bean, K. E. *IEEE Trans. Electron Devices* **1978**, *25*, 1185−1193.
(181) Palik, E. D.; Gray, H. F.; Klein, P. B. *J. Electrochem. Soc.* **1983**, *130* (4), 956−959.
(182) Jo, S.-B.; Lee, M.-W.; Lee, S.-G.; Lee, E.-H.; Park, S.-G.; O, B.-H. *J. Vac. Sci. Technol., A* **2005**, *23* (4), 905−910.
(183) Zhang, P.; Tevaarwerk, E.; Park, B. N.; Savage, D. E.; Celler, G. K.; Knezevic, I.; Evans, P. G.; Eriksson, M. A.; Lagally, M. G. *Nature* **2006**, *439* (7077), 703−6.
(184) Yoon, J.; Jo, S.; Chun, I. S.; Jung, I.; Kim, H. S.; Meitl, M.; Menard, E.; Li, X.; Coleman, J. J.; Paik, U.; Rogers, J. A. *Nature* **2010**, *465* (7296), 329−33.
(185) Smith, J. M. *MRS Bull.* **2012**, *37* (09), 794−795.
(186) Konagai, M.; Sugimoto, M.; Takahashi, K. *J. Cryst. Growth* **1978**, *45* (0), 277−280.
(187) Yablonovitch, E.; Hwang, D. M.; Gmitter, T. J.; Florez, L. T.; Harbison, J. P. *Appl. Phys. Lett.* **1990**, *56* (24), 2419−2421.
(188) Schermer, J. J.; Bauhuis, G. J.; Mulder, P.; Meulemeesters, W. J.; Haverkamp, E.; Voncken, M. M. A. J.; Larsen, P. K. *Appl. Phys. Lett.* **2000**, *76* (15), 2131−2133.
(189) Voncken, M. M. A. J.; Schermer, J. J.; Maduro, G.; Bauhuis, G. J.; Mulder, P.; Larsen, P. K. *Mater. Sci. Eng., B* **2002**, *95* (3), 242−248.
(190) Bauhuis, G. J.; Mulder, P.; Schermer, J. J. High-Efficiency Solar Cells. *Springer Ser. Mater. Sci.* **2014**, *190*, 623−643, .
(191) van Niftrik, A. T. J.; Schermer, J. J.; Bauhuis, G. J.; Mulder, P.; Larsen, P. K.; van Setten, M. J.; Attema, J. J.; Tan, N. C. G.; Kelly, J. J. *J. Electrochem. Soc.* **2008**, *155* (1), D35−D39.
(192) Smeenk, N. J.; Engel, J.; Mulder, P.; Bauhuis, G. J.; Bissels, G. M. M. W.; Schermer, J. J.; Vlieg, E.; Kelly, J. J. *ECS J. Solid State Sci. Technol.* **2013**, *2* (3), P58−P65.
(193) Prinz, V. Y.; Seleznev, V. A.; Gutakovsky, A. K.; Chehovskiy, A. V.; Preobrazhenskii, V. V.; Putyato, M. A.; Gavrilova, T. A. *Phys. E* **2000**, *6* (1), 828−831.
(194) Chun, I. S.; Verma, V. B.; Elarde, V. C.; Kim, S. W.; Zuo, J. M.; Coleman, J. J.; Li, X. *J. Cryst. Growth* **2008**, *310* (7), 2353−2358.
(195) Yu, M.; Huang, M.; Savage, D. E.; Lagally, M. G.; Blick, R. H. *IEEE Trans. Nanotechnol.* **2011**, *10* (1), 21−25.
(196) Yan, Z.; Han, M.; Shi, Y.; Badea, A.; Yang, Y.; Kulkarni, A.; Hanson, E.; Kandel, M. E.; Wen, X.; Zhang, F.; Luo, Y.; Lin, Q.; Zhang, H.; Guo, X.; Huang, Y.; Nan, K.; Jia, S.; Oraham, A. W.; Mevis, M. B.; Lim, J.; Guo, X.; Gao, M.; Ryu, W.; Yu, K. J.; Nicolau, B. G.; Petronico, A.; Rubakhin, S. S.; Lou, J.; Ajayan, P. M.; Thornton, K.; Popescu, G.; Fang, D.; Sweedler, J. V.; Braun, P. V.; Zhang, H.; Nuzzo, R. G.; Huang, Y.; Zhang, Y.; Rogers, J. A. *Proc. Natl. Acad. Sci. U. S. A.* **2017**, *114* (45), E9455−E9464.
(197) Zhou, H.; Seo, J. H.; Paskiewicz, D. M.; Zhu, Y.; Celler, G. K.; Voyles, P. M.; Zhou, W.; Lagally, M. G.; Ma, Z. *Sci. Rep.* **2013**, *3*, 1291.
(198) Paskiewicz, D. M.; Savage, D. E.; Holt, M. V.; Evans, P. G.; Lagally, M. G. *Sci. Rep.* **2015**, *4*, 4218.
(199) Durmaz, H.; Sookchoo, P.; Cui, X.; Jacobson, R. B.; Savage, D. E.; Lagally, M. G.; Paiella, R. *ACS Photonics* **2016**, *3* (10), 1978−1985.
(200) Liu, C.-C.; Jiang, H.; Yao, Y. *Phys. Rev. B: Condens. Matter Mater. Phys.* **2011**, *84* (19), 195430.
(201) Jang, H.; Wood, J. D.; Ryder, C. R.; Hersam, M. C.; Cahill, D. G. *Adv. Mater.* **2015**, *27* (48), 8017−8022.
(202) Ling, X.; Huang, S.; Hasdeo, E. H.; Liang, L.; Parkin, W. M.; Tatsumi, Y.; Nugraha, A. R. T.; Puretzky, A. A.; Das, P. M.; Sumpter, B. G.; Geohegan, D. B.; Kong, J.; Saito, R.; Drndic, M.; Meunier, V.; Dresselhaus, M. S. *Nano Lett.* **2016**, *16* (4), 2260−2267.
(203) Tran, V.; Soklaski, R.; Liang, Y.; Yang, L. *Phys. Rev. B: Condens. Matter Mater. Phys.* **2014**, *89* (23), 235319.
(204) Qiao, J.; Kong, X.; Hu, Z.-X.; Yang, F.; Ji, W. *Nat. Commun.* **2014**, *5*, 4475.
(205) Fei, R.; Faghaninia, A.; Soklaski, R.; Yan, J.-A.; Lo, C.; Yang, L. *Nano Lett.* **2014**, *14* (11), 6393−6399.
(206) Shao, Z.-G.; Ye, X.-S.; Yang, L.; Wang, C.-L. *J. Appl. Phys.* **2013**, *114* (9), 093712.
(207) Al-Dirini, F.; Hossain, F. M.; Mohammed, M. A.; Nirmalathas, A.; Skafidas, E. *Sci. Rep.* **2015**, *5*, 14815.
(208) Wang, H.; Yu, L.; Lee, Y.-H.; Shi, Y.; Hsu, A.; Chin, M. L.; Li, L.-J.; Dubey, M.; Kong, J.; Palacios, T. *Nano Lett.* **2012**, *12* (9), 4674−4680.
(209) Dai, Z.; Wang, Z.; He, X.; Zhang, X.-X.; Alshareef, H. N. *Adv. Funct. Mater.* **2017**, *27* (41), 1703119.
(210) Larentis, S.; Fallahazad, B.; Tutuc, E. *Appl. Phys. Lett.* **2012**, *101* (22), 223104.
(211) Pu, J.; Yomogida, Y.; Liu, K.-K.; Li, L.-J.; Iwasa, Y.; Takenobu, T. *Nano Lett.* **2012**, *12* (8), 4013−4017.
(212) Pu, J.; Zhang, Y.; Wada, Y.; Tse-Wei Wang, J.; Li, L.-J.; Iwasa, Y.; Takenobu, T. *Appl. Phys. Lett.* **2013**, *103* (2), 023505.
(213) Senthilkumar, V.; Tam, L. C.; Kim, Y. S.; Sim, Y.; Seong, M.-J.; Jang, J. I. *Nano Res.* **2014**, *7* (12), 1759−1768.
(214) Wang, H.; Wang, X.; Xia, F.; Wang, L.; Jiang, H.; Xia, Q.; Chin, M. L.; Dubey, M.; Han, S.-j. *Nano Lett.* **2014**, *14* (11), 6424−6429.
(215) Yu, X.; Sivula, K. *ACS Energy Letters* **2016**, *1* (1), 315−322.
(216) Zhang, K.; Bersch, B. M.; Joshi, J.; Addou, R.; Cormier, C. R.; Zhang, C.; Xu, K.; Briggs, N. C.; Wang, K.; Subramanian, S.; Cho, K.; Fullerton-Shirey, S.; Wallace, R. M.; Vora, P. M.; Robinson, J. A. *Adv. Funct. Mater.* **2018**, *28*, 1706950.
(217) Shanmugam, M.; Durcan, C. A.; Yu, B. *Nanoscale* **2012**, *4* (23), 7399−405.

DOI: 10.1021/jacs.8b04225
J. Am. Chem. Soc. 2018, 140, 9001−9019

(218) Khan, M. A.; Rathi, S.; Lim, D.; Yun, S. J.; Youn, D.-H.; Watanabe, K.; Taniguchi, T.; Kim, G.-H. *Chem. Mater.* **2018**, *30* (3), 1011−1016.
(219) Buscema, M.; Groenendijk, D. J.; Blanter, S. I.; Steele, G. A.; van der Zant, H. S. J.; Castellanos-Gomez, A. *Nano Lett.* **2014**, *14* (6), 3347−3352.
(220) Buscema, M.; Groenendijk, D. J.; Steele, G. A.; van der Zant, H. S. J.; Castellanos-Gomez, A. *Nat. Commun.* **2014**, *5*, 4651.
(221) Wu, J. Y.; Chun, Y. T.; Li, S.; Zhang, T.; Wang, J.; Shrestha, P. K.; Chu, D. *Adv. Mater.* **2018**, *30* (7), 1705880.
(222) Britnell, L.; Ribeiro, R. M.; Eckmann, A.; Jalil, R.; Belle, B. D.; Mishchenko, A.; Kim, Y.-J.; Gorbachev, R. V.; Georgiou, T.; Morozov, S. V.; Grigorenko, A. N.; Geim, A. K.; Casiraghi, C.; Neto, A. H. C.; Novoselov, K. S. *Science* **2013**, *340* (6138), 1311−1314.
(223) Youngblood, N.; Chen, C.; Koester, S. J.; Li, M. *Nat. Photonics* **2015**, *9*, 247−252.
(224) Gao, G.; Wan, B.; Liu, X.; Sun, Q.; Yang, X.; Wang, L.; Pan, C.; Wang, Z. L. *Adv. Mater.* **2018**, *30*, 1705088.
(225) Lee, W.; Liu, Y.; Lee, Y.; Sharma, B. K.; Shinde, S. M.; Kim, S. D.; Nan, K.; Yan, Z.; Han, M.; Huang, Y.; Zhang, Y.; Ahn, J.-H.; Rogers, J. A. *Nat. Commun.* **2018**, *9*, 1417.
(226) Choi, C.; Choi, M. K.; Liu, S.; Kim, M. S.; Park, O. K.; Im, C.; Kim, J.; Qin, X.; Lee, G. J.; Cho, K. W.; Kim, M.; Joh, E.; Lee, J.; Son, D.; Kwon, S.-H.; Jeon, N. L.; Song, Y. M.; Lu, N.; Kim, D.-H. *Nat. Commun.* **2017**, *8* (1), 1664.
(227) Hsu, K. F.; Loo, S.; Guo, F.; Chen, W.; Dyck, J. S.; Uher, C.; Hogan, T.; Polychroniadis, E. K.; Kanatzidis, M. G. *Science* **2004**, *303* (5659), 818−821.
(228) Biswas, K.; He, J.; Blum, I. D.; Wu, C.-I.; Hogan, T. P.; Seidman, D. N.; Dravid, V. P.; Kanatzidis, M. G. *Nature* **2012**, *489* (7416), 414−418.
(229) Rhyee, J.-S.; Lee, K. H.; Lee, S. M.; Cho, E.; Kim, S. I.; Lee, E.; Kwon, Y. S.; Shim, J. H.; Kotliar, G. *Nature* **2009**, *459* (7249), 965−968.
(230) Zhao, L.-D.; Dravid, V. P.; Kanatzidis, M. G. *Energy Environ. Sci.* **2014**, *7* (1), 251−268.
(231) Feng, X.; Meitl, M. A.; Bowen, A. M.; Huang, Y.; Nuzzo, R. G.; Rogers, J. A. *Langmuir* **2007**, *23* (25), 12555−12560.
(232) Lee, K. J.; Motala, M. J.; Meitl, M. A.; Childs, W. R.; Menard, E.; Shim, A. K.; Rogers, J. A.; Nuzzo, R. G. *Adv. Mater.* **2005**, *17*, 2332−2336.
(233) Carlson, A.; Wang, S. D.; Elvikis, P.; Ferreira, P. M.; Huang, Y. G.; Rogers, J. A. *Adv. Funct. Mater.* **2012**, *22* (21), 4476−4484.
(234) Carlson, A.; Kim-Lee, H. J.; Wu, J.; Elvikis, P.; Cheng, H. Y.; Kovalsky, A.; Elgan, S.; Yu, Q. M.; Ferreira, P. M.; Huang, Y. G.; Turner, K. T.; Rogers, J. A. *Appl. Phys. Lett.* **2011**, *98* (26), 264104.
(235) Meitl, M. A.; Zhu, Z. T.; Kumar, V.; Lee, K. J.; Feng, X.; Huang, Y. Y.; Adesida, I.; Nuzzo, R. G.; Rogers, J. A. *Nat. Mater.* **2006**, *5* (1), 33−38.
(236) Carlson, A.; Bowen, A. M.; Huang, Y.; Nuzzo, R. G.; Rogers, J. A. *Adv. Mater.* **2012**, *24* (39), 5284−5318.
(237) Kim, S.; Wu, J.; Carlson, A.; Jin, S. H.; Kovalsky, A.; Glass, P.; Liu, Z.; Ahmed, N.; Elgan, S. L.; Chen, W.; Ferreira, P. M.; Sitti, M.; Huang, Y.; Rogers, J. A. *Proc. Natl. Acad. Sci. U. S. A.* **2010**, *107* (40), 17095−100.
(238) Sun, Y. G.; Choi, W. M.; Jiang, H. Q.; Huang, Y. G. Y.; Rogers, J. A. *Nat. Nanotechnol.* **2006**, *1* (3), 201−207.
(239) Kim, D.-H.; Song, J.; Choi, W. M.; Kim, H.-S.; Kim, R.-H.; Liu, Z.; Huang, Y. Y.; Hwang, K.-C.; Zhang, Y.-w.; Rogers, J. A. *Proc. Natl. Acad. Sci. U. S. A.* **2008**, *105* (48), 18675−18680.
(240) Xu, S.; Yan, Z.; Jang, K.; Huang, W.; Fu, H.; Kim, J.; Wei, Z.; Flavin, M.; McCracken, J.; Wang, R.; Badea, A.; Liu, Y.; Xiao, D.; Zhou, G.; Lee, J.; Chung, H.; Cheng, H.; Ren, W.; Banks, A.; Li, X.; Paik, U.; Nuzzo, R. G.; Huang, Y.; Zhang, Y.; Rogers, J. A. *Science* **2015**, *347* (6218), 154−159.
(241) Zhang, Y.; Yan, Z.; Nan, K.; Xiao, D.; Liu, Y.; Luan, H.; Fu, H.; Wang, X.; Yang, Q.; Wang, J.; Ren, W.; Si, H.; Liu, F.; Yang, L.; Li, H.; Wang, J.; Guo, X.; Luo, H.; Wang, L.; Huang, Y.; Rogers, J. A. *Proc. Natl. Acad. Sci. U. S. A.* **2015**, *112* (38), 11757−11764.
(242) Yan, Z.; Zhang, F.; Liu, F.; Han, M.; Ou, D.; Liu, Y.; Lin, Q.; Guo, X.; Fu, H.; Xie, Z.; Gao, M.; Huang, Y.; Kim, J.; Qiu, Y.; Nan, K.; Kim, J.; Gutruf, P.; Luo, H.; Zhao, A.; Hwang, K.-C.; Huang, Y.; Zhang, Y.; Rogers, J. A. *Sci. Adv.* **2016**, *2* (9), No. e1601014.
(243) Zhang, K.; Jung, Y. H.; Mikael, S.; Seo, J.-H.; Kim, M.; Mi, H.; Zhou, H.; Xia, Z.; Zhou, W.; Gong, S.; Ma, Z. *Nat. Commun.* **2017**, *8* (1), 1782.
(244) McCracken, J. M.; Xu, S.; Badea, A.; Jang, K.-I.; Yan, Z.; Wetzel, D. J.; Nan, K.; Lin, Q.; Han, M.; Anderson, M. A.; Lee, J. W.; Wei, Z.; Pharr, M.; Wang, R.; Su, J.; Rubakhin, S. S.; Sweedler, J. V.; Rogers, J. A.; Nuzzo, R. G. *Adv. Biosys.* **2017**, *1* (9), 1700068.
(245) Jang, K.-I.; Li, K.; Chung, H. U.; Xu, S.; Jung, H. N.; Yang, Y.; Kwak, J. W.; Jung, H. H.; Song, J.; Yang, C.; Wang, A.; Liu, Z.; Lee, J. Y.; Kim, B. H.; Kim, J.-H.; Lee, J.; Yu, Y.; Kim, B. J.; Jang, H.; Yu, K. J.; Kim, J.; Lee, J. W.; Jeong, J.-W.; Song, Y. M.; Huang, Y.; Zhang, Y.; Rogers, J. A. *Nat. Commun.* **2017**, *8*, 15894.
(246) Fu, H.; Nan, K.; Bai, W.; Huang, W.; Bai, K.; Lu, L.; Zhou, C.; Liu, Y.; Liu, F.; Wang, J.; Han, M.; Yan, Z.; Luan, H.; Zhang, Y.; Zhang, Y.; Zhao, J.; Cheng, X.; Li, M.; Lee, J. W.; Liu, Y.; Fang, D.; Li, X.; Huang, Y.; Zhang, Y.; Rogers, J. A. *Nat. Mater.* **2018**, *17* (3), 268−276.
(247) Kang, S.-K.; Murphy, R. K. J.; Hwang, S.-W.; Lee, S. M.; Harburg, D. V.; Krueger, N. A.; Shin, J.; Gamble, P.; Cheng, H.; Yu, S.; Liu, Z.; McCall, J. G.; Stephen, M.; Ying, H.; Kim, J.; Park, G.; Webb, R. C.; Lee, C. H.; Chung, S.; Wie, D. S.; Gujar, A. D.; Vemulapalli, B.; Kim, A. H.; Lee, K.-M.; Cheng, J.; Huang, Y.; Lee, S. H.; Braun, P. V.; Ray, W. Z.; Rogers, J. A. *Nature* **2016**, *530* (7588), 71−76.
(248) Yu, K. J.; Kuzum, D.; Hwang, S.-W.; Kim, B. H.; Juul, H.; Kim, N. H.; Won, S. M.; Chiang, K.; Trumpis, M.; Richardson, A. G.; Cheng, H.; Fang, H.; Thompson, M.; Bink, H.; Talos, D.; Seo, K. J.; Lee, H. N.; Kang, S.-K.; Kim, J.-H.; Lee, J. Y.; Huang, Y.; Jensen, F. E.; Dichter, M. A.; Lucas, T. H.; Viventi, J.; Litt, B.; Rogers, J. A. *Nat. Mater.* **2016**, *15*, 782−792.
(249) Chang, J.-K.; Fang, H.; Bower, C. A.; Song, E.; Yu, X.; Rogers, J. A. *Proc. Natl. Acad. Sci. U. S. A.* **2017**, *114* (28), E5522−E5529.
(250) Chang, J. K.; Chang, H. P.; Guo, Q.; Koo, J.; Wu, C. I.; Rogers, J. A. *Adv. Mater.* **2018**, *30* (11), 1704955.
(251) Fang, H.; Yu, K. J.; Gloschat, C.; Yang, Z.; Song, E.; Chiang, C.-H.; Zhao, J.; Won, S. M.; Xu, S.; Trumpis, M.; Zhong, Y.; Han, S. W.; Xue, Y.; Xu, D.; Choi, S. W.; Cauwenberghs, G.; Kay, M.; Huang, Y.; Viventi, J.; Efimov, I. R.; Rogers, J. A. *Nature Biomedical Engineering* **2017**, *1*, 0038.
(252) Xu, L.; Gutbrod, S. R.; Bonifas, A. P.; Su, Y.; Sulkin, M. S.; Lu, N.; Chung, H.-J.; Jang, K.-I.; Liu, Z.; Ying, M.; Lu, C.; Webb, R. C.; Kim, J.-S.; Laughner, J. I.; Cheng, H.; Liu, Y.; Ameen, A.; Jeong, J.-W.; Kim, G.-T.; Huang, Y.; Efimov, I. R.; Rogers, J. A. *Nat. Commun.* **2014**, *5*, 3329.
(253) Kim, T.-i.; Jung, Y. H.; Song, J.; Kim, D.; Li, Y.; Kim, H.-s.; Song, I.-S.; Wierer, J. J.; Pao, H. A.; Huang, Y.; Rogers, J. A. *Small* **2012**, *8* (11), 1643−1649.
(254) Song, Y. M.; Xie, Y.; Malyarchuk, V.; Xiao, J.; Jung, I.; Choi, K.-J.; Liu, Z.; Park, H.; Lu, C.; Kim, R.-H.; Li, R.; Crozier, K. B.; Huang, Y.; Rogers, J. A. *Nature* **2013**, *497* (7447), 95−99.
(255) Polman, A.; Atwater, H. A. *Nat. Mater.* **2012**, *11* (3), 174−7.
(256) Xiong, K.; Mi, H.; Chang, T. H.; Liu, D.; Xia, Z.; Wu, M. Y.; Yin, X.; Gong, S.; Zhou, W.; Shin, J. C.; Li, X.; Arnold, M.; Wang, X.; Yuan, H. C.; Ma, Z. *Energy Sci. Eng.* **2018**, *6* (1), 47−55.
(257) Yoon, J.; Baca, A. J.; Park, S. I.; Elvikis, P.; Geddes, J. B., 3rd; Li, L.; Kim, R. H.; Xiao, J.; Wang, S.; Kim, T. H.; Motala, M. J.; Ahn, B. Y.; Duoss, E. B.; Lewis, J. A.; Nuzzo, R. G.; Ferreira, P. M.; Huang, Y.; Rockett, A.; Rogers, J. A. *Nat. Mater.* **2008**, *7* (11), 907−15.
(258) Kosten, E. D.; Atwater, J. H.; Parsons, J.; Polman, A.; Atwater, H. A. *Light: Sci. Appl.* **2013**, *2*, No. e45.
(259) Miller, O. D.; Yablonovitch, E.; Kurtz, S. R. *IEEE Journal of Photovoltaics* **2012**, *2* (3), 303−311.
(260) Sheng, X.; Bower, C. A.; Bonafede, S.; Wilson, J. W.; Fisher, B.; Meitl, M.; Yuen, H.; Wang, S.; Shen, L.; Banks, A. R.; Corcoran, C.

DOI: 10.1021/jacs.8b04225
J. Am. Chem. Soc. 2018, 140, 9001−9019

J.; Nuzzo, R. G.; Burroughs, S.; Rogers, J. A. *Nat. Mater.* **2014**, *13* (6), 593−598.
(261) Kosten, E. D.; Kayes, B. M.; Atwater, H. A. *Energy Environ. Sci.* **2014**, *7* (6), 1907.
(262) Sheng, X.; Yun, M. H.; Zhang, C.; Al-Okaily, A. a. M.; Masouraki, M.; Shen, L.; Wang, S.; Wilson, W. L.; Kim, J. Y.; Ferreira, P.; Li, X.; Yablonovitch, E.; Rogers, J. A. *Adv. Energy Mater.* **2015**, *5* (1), 1400919.
(263) Yamaguchi, M. *Phys. E* **2002**, *14* (1−2), 84−90.
(264) Guo, X.; Li, H.; Yeop Ahn, B.; Duoss, E. B.; Hsia, K. J.; Lewis, J. A.; Nuzzo, R. G. *Proc. Natl. Acad. Sci. U. S. A.* **2009**, *106* (48), 20149−20154.
(265) Yoon, J.; Li, L.; Semichaevsky, A. V.; Ryu, J. H.; Johnson, H. T.; Nuzzo, R. G.; Rogers, J. A. *Nat. Commun.* **2011**, *2*, 343.
(266) Baca, A. J.; Yu, K. J.; Xiao, J.; Wang, S.; Yoon, J.; Ryu, J. H.; Stevenson, D.; Nuzzo, R. G.; Rockett, A. A.; Huang, Y.; Rogers, J. A. *Energy Environ. Sci.* **2010**, *3* (2), 208−211.
(267) Luque, A.; Andreev, V. *Concentrator Photovoltaics*; Springer, 2007.
(268) Nelson, J. *The Physics of Solar Cells*; Imperial College Press: London, 2003.
(269) *The Handbook of Photovoltaics Science and Engineering*, 2nd ed.; John Wiley & Sons, Ltd., 2011.
(270) Yao, Y.; Lee, K.-T.; Sheng, X.; Batara, N. A.; Hong, N.; He, J.; Xu, L.; Hussain, M. M.; Atwater, H. A.; Lewis, N. S.; Nuzzo, R. G.; Rogers, J. A. *Adv. Energy Mater.* **2017**, *7* (7), 1601992.
(271) Xia, Z.; Song, H.; Kim, M.; Zhou, M.; Chang, T.-H.; Liu, D.; Yin, X.; Xiong, K.; Mi, H.; Wang, X.; Xia, F.; Yu, Z.; Ma, Z.; Gan, Q. *Sci. Adv.* **2017**, *3* (7), No. e1602783.
(272) Zhao, D.; Liu, S.; Yang, H.; Ma, Z.; Reuterskiöld-Hedlund, C.; Hammar, M.; Zhou, W. *Sci. Rep.* **2016**, *6*, 18860.
(273) Ko, H.; Takei, K.; Kapadia, R.; Chuang, S.; Fang, H.; Leu, P. W.; Ganapathi, K.; Plis, E.; Kim, H. S.; Chen, S.-Y.; Madsen, M.; Ford, A. C.; Chueh, Y.-L.; Krishna, S.; Salahuddin, S.; Javey, A. *Nature* **2010**, *468* (7321), 286−289.
(274) Pillarisetty, R.; Chu-Kung, B.; Corcoran, S.; Dewey, G.; Kavalieros, J.; Kennel, H.; Kotlyar, R.; Le, V.; Lionberger, D.; Metz, M.; Mukherjee, N.; Nah, J.; Rachmady, W.; Radosavljevic, M.; Shah, U.; Taft, S.; Then, H.; Zelick, N.; Chau, R. *2010 IEEE International Electron Devices Meeting (IEDM)* **2010**, 6.7.1−6.7.4.
(275) Nainani, A.; Irisawa, T.; Yuan, Z.; Sun, Y.; Krishnamohan, T.; Reason, M.; Bennett, B. R.; Boos, J. B.; Ancona, M. G.; Nishi, Y.; Saraswat, K. C. Development of high-k dielectric for antimonides and a sub 350°C III-V pMOSFET outperforming Germanium. *2010 International Electron Devices Meeting*, San Francisco, CA, December 6−8, 2010; pp 6.4.1−6.4.4.
(276) Koitmäe, A.; Harberts, J.; Loers, G.; Müller, M.; Bausch, C. S.; Sonnenberg, D.; Heyn, C.; Zierold, R.; Hansen, W.; Blick, R. H. *Adv. Mater. Interfaces* **2016**, *3* (24), 1600746.
(277) ElAfandy, R. T.; AbuElela, A. F.; Mishra, P.; Janjua, B.; Oubei, H. M.; Büttner, U.; Majid, M. A.; Ng, T. K.; Merzaban, J. S.; Ooi, B. S. *Small* **2017**, *13* (7), 1603080.
(278) Schulze, S.; Huang, G.; Krause, M.; Aubyn, D.; Quiñones, V. A. B.; Schmidt, C. K.; Mei, Y.; Schmidt, O. G. *Adv. Eng. Mater.* **2010**, *12* (9), B558−B564.
(279) Spira, M. E.; Hai, A. *Nat. Nanotechnol.* **2013**, *8* (2), 83−94.
(280) Robinson, J. T.; Jorgolli, M.; Shalek, A. K.; Yoon, M.-H.; Gertner, R. S.; Park, H. *Nat. Nanotechnol.* **2012**, *7* (3), 180−184.
(281) Bakkum, D. J.; Frey, U.; Radivojevic, M.; Russell, T. L.; Müller, J.; Fiscella, M.; Takahashi, H.; Hierlemann, A. *Nat. Commun.* **2013**, *4*, 2181.
(282) Medina-Sánchez, M.; Ibarlucea, B.; Pérez, N.; Karnaushenko, D. D.; Weiz, S. M.; Baraban, L.; Cuniberti, G.; Schmidt, O. G. *Nano Lett.* **2016**, *16* (7), 4288−4296.
(283) Fujie, T.; Ahadian, S.; Liu, H.; Chang, H.; Ostrovidov, S.; Wu, H.; Bae, H.; Nakajima, K.; Kaji, H.; Khademhosseini, A. *Nano Lett.* **2013**, *13* (7), 3185−92.
(284) Tian, B.; Liu, J.; Dvir, T.; Jin, L.; Tsui, J. H.; Qing, Q.; Suo, Z.; Langer, R.; Kohane, D. S.; Lieber, C. M. *Nat. Mater.* **2012**, *11* (11), 986−94.
(285) Xi, W.; Schmidt, C. K.; Sanchez, S.; Gracias, D. H.; Carazo-Salas, R. E.; Jackson, S. P.; Schmidt, O. G. *Nano Lett.* **2014**, *14* (8), 4197−204.
(286) Nguyen, A. T.; Sathe, S. R.; Yim, E. K. F. *J. Phys.: Condens. Matter* **2016**, *28* (18), 183001.
(287) Wu, G.-H.; Hsu, S.-h. *Journal of Medical and Biological Engineering* **2015**, *35* (3), 285−292.

DOI: 10.1021/jacs.8b04225
J. Am. Chem. Soc. 2018, 140, 9001−9019